Meteoritics & Planetary Science 40, Nr 9/10, 1473–1492 (2005)
Abstract available online at http://meteoritics.org

Target rocks, impact glasses, and melt rocks from the Lonar impact crater, India: Petrography and geochemistry

Shiloh OSAE[1, 2], Saumitra MISRA[3], Christian KOEBERL[1*], Debashish SENGUPTA[3], and Sambhunath GHOSH[4]

[1]Department of Geological Sciences, University of Vienna, Althanstrasse 14, A-1090 Vienna, Austria
[2]National Nuclear Research Institute, Ghana Atomic Energy Commission, P.O. Box LG 80, Legon-Accra, Ghana
[3]Department of Geology and Geophysics, Indian Institute of Technology, Kharagpur 721 302, India
[4]Geological Survey of India, 27 Jawaharlal Nehru Road, Kolkata 700016, India
*Corresponding author. E-mail: christian.koeberl@univie.ac.at

(Received 01 February 2005; revision accepted 16 July 2005)

Abstract–The Lonar crater, India, is the only well-preserved simple crater on Earth in continental flood basalts; it is excavated in the Deccan trap basalts of Cretaceous-Tertiary age. A representative set of target basalts, including the basalt flows excavated by the crater, and a variety of impact breccias and impact glasses, were analyzed for their major and trace element compositions. Impact glasses and breccias were found inside and outside the crater rim in a variety of morphological forms and shapes. Comparable geochemical patterns of immobile elements (e.g., REEs) for glass, melt rock and basalt indicates minimal fractionation between the target rocks and the impactites. We found only little indication of post-impact hydrothermal alteration in terms of volatile trace element changes. No clear indication of an extraterrestrial component was found in any of our breccias and impact glasses, indicating either a low level of contamination, or a non-chondritic or otherwise iridium-poor impactor.

INTRODUCTION AND HISTORY OF STUDIES

The Lonar crater (centered at 19°59′ N and 76°31′ E), in the Buldana District, Maharashtra, India (Fig. 1a), is located in the Deccan Traps. It has an average diameter of 1830 m and a depth of about 150 m, with a saline lake occupying the floor of the crater (e.g., Nandy and Deo 1961; Chowdhury and Handa 1978; Nayak 1985). The rim of the crater is raised about 20 m above the surrounding plain. Lonar is the only well-known example of an impact into a (continental) flood basalt terrain and potentially offers an analogue for impacts on basaltic terrains on the other terrestrial planets and terrestrial planet-like bodies, e.g., martian impact sites in the Tharsis region. The origin of this crater has been a matter of controversy since the 19th century when geoscientists first started studying the crater. In one of the earliest descriptions, Malcolmson (1840) suggested that Lonar might be "the only instance of a volcanic outburst discovered in this immense volcanic region," while Newbold (1844) concluded, "from the absence of any streams of lava, and of the quaquaversal dip attending craters of elevation, I am inclined to believe it to have been occasioned by subsidence . . . or by a great gaseous extrication." In the 20th century, the hypothesis of a volcanic origin was still quoted (e.g., Nandy and Deo 1961), while the first suggestion that Lonar Crater was formed by meteoritic impact seems to have been made by Lafond and Dietz (1964). Even in the past 20 years, a "crypto-volcanic" origin associated with deep-seated carbonatites was promulgated (e.g., Subrahmanyam 1985; Mishra 1987). However, there is now abundant evidence in support of an impact origin of this crater, including the relative youthfulness of the crater (in comparison to the age of regional volcanism), its morphology, the presence of glasses around the crater, ejected melt breccias with shocked minerals, and a subsurface breccia identified in drill cores beneath the crater (e.g., Nayak 1972; Fredriksson et al. 1973, 1979; Fudali et al. 1980).

A shallow depression, known as Little Lonar, which has a diameter of about 300 m and a raised rim of about 20 m above the surrounding plain along the western and southern rim of this depression, occurs ~700 m north of Lonar Crater (Fig. 1b). It has been suggested that this structure formed together with Lonar Crater, perhaps by a fragment of the same impactor (Fredriksson et al. 1973). However, no confirmation of this suggestion has been obtained so far.

Fudali et al. (1980), using detailed gravity measurements and morphological data, reconstructed the pre-erosional dimensions of Lonar Crater. According to them, the original diameter of the crater was 1710 m, with an average rim height

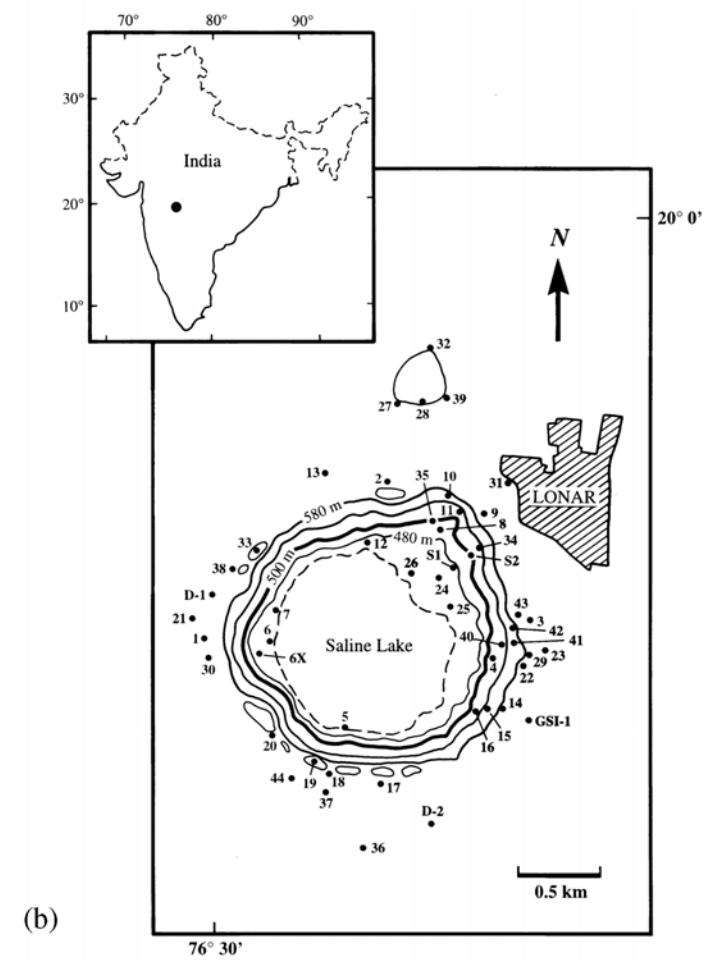

Fig. 1. a) Panoramic view of Lonar crater, from the east side; b) map of Lonar area, showing Lonar Crater Lake and the locations of the samples taken for the present study. The government rest house is located a few meters east of location 43.

of ~40 m, including 30–35 m of rim rock uplift, 5–10 m of ejecta, and a depth of 230–245 m from the rim crest to the crater floor.

In the 1970s, the Geological Survey of India, in collaboration with the Smithsonian Institution, USA, drilled five boreholes within the crater lake, penetrating into the crater floor. After drilling through ~100 m of lake sediments, coarse blocks of breccia up to several meters in size were encountered (Fredriksson et al. 1973). These large blocks were either unshocked or only slightly shocked. In the core drilled in the center of the crater (i.e., LNR 2; see Fig. 2 of Fredriksson et al. [1973]), moderately to strongly shocked microbreccia (with clasts several cm in size) were encountered in the depth interval from 305 to 355 m below the

lake floor (Fredriksson et al. 1973). Also, three meter-deep trenches dug during this collaborative work revealed abundant evidence of shock metamorphism (in plagioclase, feldspar, and other minerals in the basalt; Fredriksson et al. 1973, 1979).

Though it was established that Lonar Crater is a meteorite impact crater, neither the detailed geochemistry of the varieties of impact melt breccia and glass occurring in and around this crater, nor the possible composition of the impactor, is known in any detail. Strobe et al. (1978) first published some detailed geochemistry (29 elements) of four target rock basalts and two impact melt rocks. They also noted some variation in the Cr content among the basalt and impact melt samples, but nothing was predicted on the impactor composition. Ghosh and Bhaduri (2003), in their fairly detailed geochemical study of six target rock basalt and six impact melt rock samples, showed that the latter were somewhat enriched in the abundances of Al, Fe, K, Co, and Sr, and depleted in those of Ti, Mg, Cr, and Sc, compared to the basalt compositions. However, no suggestion was given on impactor composition.

With this background, we attempt here to provide detailed field and petrographic descriptions of varieties of impact melt rocks, breccias, and spherules found in and around the Lonar Crater and present the so far largest data set of major and trace element compositions of target basalts and impact breccias and spherules. These data are used for a geochemical comparison between target and impactites, and also to provide data for the detailed classification of the Deccan basalts at Lonar.

GEOLOGICAL SETTING OF LONAR

In the Lonar area, 600–700-m-thick sub-horizontal Deccan basalt flows overlie the Precambrian basement of west-central India (Fudali et al. 1980). The Deccan Traps are one of the largest volcanic provinces in the world, consisting of more than 2-km-thick flat-lying basalt lava flows covering an area of nearly 500,000 km^2 in west-central India; estimates of the original area covered by the lava flows are as high as 1.5 million km^2, and the volume of basalt is estimated at ~0.5 million km^3 (e.g., Mahoney 1988; Cox and Hawkesworth 1985; Widdowson et al. 2000). The Deccan basalts were irrupted between ~69 and 63 Ma ago, with a main peak in activity around 66 to 65 Ma (see reviews by Pandey [2002] and Courtillot and Renne [2003]). Six basalt flows, ranging in thickness between ~8 and 40 m, are seen in and around Lonar village, while four flows are exposed on the crater wall (Ghosh and Bhaduri 2003). The flows are composed of fresh, dense basalt in the upper 50 m of the crater wall, but below this level, the flows are heavily weathered and friable (Fudali et al. 1980). The topmost (termed the sixth) flow is only exposed in two hills outside the crater rim and, thus, has not been considered any further. The basalt flows are separated by horizons of red and green paleosols, have vugs filled with secondary materials like chlorite, zeolite, quartz, and brown limonite, and most have what was interpreted by Ghosh and Bhaduri (2003) as a chill margin at their bottom and a heated and brecciated top. Widdowson et al. (1997), on the other hand, interpreted some of these features as the result of weathering. However, in most cases, the flows are difficult to identify on the crater wall due to the thick overburden and the vegetation cover. In the northern and western parts of the inner crater wall, red bole layers allow one to discern the different basaltic flows. A preliminary geological map of Lonar was recently presented by Maloof et al. (2005).

The deformation experienced by the target rocks as a result of the cratering event has been well-preserved in the upper two flows (Fudali et al. 1980). In the crater walls, the flows are upturned and, in places at the rim, even overturned. Plastic deformation and compaction in the lower parts of relatively incompetent flows are also observed. All around the circumference of the crater, except for a small sector in the northeast, there is a continuous raised rim ~20 m above the surrounding plains (Fudali et al. 1980). At the top of the rim there are large, meter to tens-of-meters sized basalt blocks that are cemented together with finer-grained material of similar composition. The uppermost basalt flow is overlain in most parts by a dense black clayey suite of paleosol that varies in thickness between 0.05 to 0.9 m (Fudali et al. 1980; Ghosh and Bhaduri 2003). This soil can also be observed beneath the outer portion of the ejecta blanket in several gullies south of the crater and is good evidence that this soil predates the formation of the crater. Moreover, its persistent presence also demonstrates that the surface morphology of Lonar Crater has not significantly changed since the cratering event. A thinner post-cratering soil profile has developed over the ejecta blanket. An almost continuous ejecta blanket exists outside the rim of Lonar Crater and varies in radial extent from ~400 m to 1600 m and in thickness from a few cm to more than 8 m (Fudali et al. 1980; Ghosh and Bhaduri 2003). Discontinuous patches of ejecta are also found as far as 3 km from the crater rim (Fudali et al. 1980). The ejecta blanket slopes very gently (2–6°) away from the crater, with a hummocky surface; it appears to represent the original surface that was not much modified by post-cratering erosion. This good state of preservation may be the result of the very gentle nature of the slope and the stabilizing cover of vegetation, and a lack of erosion noted throughout the region.

The present crater floor is covered by unconsolidated sediments and is almost flat, ranging in elevation above sea level (a.s.l.) from about 450 m near the base of the inner wall to about 468 m (Fudali et al. 1980). The maximum elevation of the crater rim is more than 600 m (a.s.l.) but is normally about 590 m. The average slope of the inner wall is 26°, and the bedrock dips away from the crater at an angle of about 8° to 20°. However, sharply bounded patches occasionally occur

where the bedrocks show overturned dip and their attitudes are approximately parallel to the rim wall slope. The black clayey pre-crater soil caps the upturned tops of the basalt sequence at about the 585 m level in the northeastern segment of the rim wall.

Ejecta located around the crater rim occur in two different forms (e.g., Fredriksson et al. 1973, 1979). Most of the ejecta deposits are crudely stratified and unshocked, and contain clasts from a mixture of different bedrock units; these ejecta extend to within 1½ crater radii distance from the crater rim (e.g., Ghosh and Bhaduri 2003). A discontinuous overlying layer up to a meter thick is present in some places, which has clasts that are unshocked or show a range of shock effects up to intensely shocked varieties (e.g., planar deformation features in plagioclase and pyroxene and the presence of the high-pressure polymorph maskelynite; Kieffer et al. 1976) and extends for ~½ crater radii km from the crater rim (see Fudali et al. 1980; Ghosh and Bhaduri 2003). Impact-derived melt rock fragments and glasses are common in the ejecta deposits up to about a crater radius from the crater rim and in the soil that is probably derived from the weathering of the ejecta (Nayak 1972; Fredriksson et al. 1973; Ghosh and Bhaduri 2003). Additionally, tektite-like glasses, about 10 to 15 cm in diameter, have also been reported in the ejecta blanket (Sengupta 1986). The glass-bearing breccia outside the crater rim was recently studied and suggested to be the basaltic equivalent of a suevitic breccia (Koeberl et al. 2004). Although the data clearly indicate that Lonar was formed by the impact of a meteorite, no impactor fragments have yet been found within or around the crater.

The age of the impact event itself is, so far, not well-constrained, while the age of the target area is sufficiently well-known (the main activity of the Deccan Trap eruptions was about 65 million years ago. There is no doubt that the crater is very young compared to the age of the Deccan basalts (which presents a fatal problem to the cryptoexplosion and volcanic origin hypotheses, because the volcanic activity in the area had ceased tens of millions of years before the crater formation). Several possible impact dates have been reported in the literature, but they are either not well-documented or do not agree with each other. Fredriksson et al. (1973) reported a preliminary fission track age of less than 50,000 yr for Lonar impact glasses. Radiocarbon ages of post-impact lake sediments gave radiocarbon ages of ~15–30 ka (unpublished data; see Fredriksson et al. 1979; Sengupta 1986; Sengupta et al. 1997), which were thought to be lower age limits for the impact event due to contamination with young carbon. Sengupta and Bhandari (1988) quoted a thermoluminescence age of 62 ka. Based on more or less the same data set, Sengupta et al. (1997) reported an age of 52 ± 8 ka. More recently, Storzer and Koeberl (2004) reported a fission-track age of only 15 ka, but with a very high error due to the low number of tracks counted. Thus, the age of Lonar is only constrained between ~15 and 50 ka, similar to the age of the similar sized Meteor Crater in Arizona. However, remote sensing studies indicate that Lonar is in a slightly more degraded condition than Meteor Crater (Grant and Schultz 1993; Grant 1999), but this could also be due to a different weathering rate.

In terms of terrestrial impact craters the importance of Lonar Crater is that it is the only well-preserved simple crater in continental flood basalt and one of only very few in basaltic target rock in general (Nayak 1972; Fredriksson et al. 1973). The 20-km-diameter Logancha crater in Russia is also situated in basalt, but only very little information is available, and only a subdued ring depression of a few hundred meters depth remains; basaltic tuffs and dolerites are the target rocks there (e.g., Feldman et al. 1983; Masaitis 1999). It is unclear if the Logancha crater actually formed in basalts of the Siberian Traps, as its coordinates place it within the extent of those flood basalts as drawn by Reichow et al. (2002), but Masaitis (1999) lists it as being situated in the central part of the lower Triassic basalt plateau. Because it provides rare ground truth for impact effects in basaltic targets, Lonar can be used as an analogue for impact craters on terrestrial planets with basaltic crusts (e.g., Mars; Hagerty and Newsom 2003). As indicated by Fudali et al. (1980), the basaltic nature of the target led to some unique formations not observed at other impact craters. Field observations indicate that a fluidized debris surge, similar to the "fluidized craters" of Mars, may be the mechanism of ejecta transportation and deposition at Lonar. This may explain the fact that only limited physical features common to other impact sites are observed at the Lonar crater site.

ANALYTICAL METHODS

For the present study, 43 samples were taken in 2000 and 2001 from within and outside Lonar crater for petrographic and geochemical analyses. This included 19 basalt samples of various flows, 17 impact melt rock, and seven impact glass samples. In some cases, trenches were dug to collect relatively fresh (unaltered) samples. Sample locations are shown in Fig. 1b; sample locations and field classification of samples are given in the Appendix. Thin sections of selected samples were studied by optical microscopy. Representative samples of target rock basalt and impact melt/breccia, weighing between ~20 to 50 g (where available), were crushed and powdered using an alumina ceramics jaw crusher and agate or alumina mills. Abundances of the major elements and selected trace elements (i.e., Rb, Sr, Y, Nb, Co, Ni, Cu, Zn, V, Cr, Ba) were determined by X-ray fluorescence spectrometry (XRF) following the procedure of Reimold et al. (1994). The contents of all other trace elements (including the rare earth elements) were determined using instrumental neutron activation analysis (INAA). Instrumentation, sample preparation techniques, and information on accuracy, precision, and

standards were described in Koeberl (1993). Samples of mm-size impact glass spherules were too small for XRF analyses and were only analyzed by INAA.

RESULTS AND DISCUSSION: PETROGRAPHY AND GEOCHEMISTRY

Country-Rock Basalt

Samples of basalt, without any visual indications of weathering or alteration, were collected mostly from the third and fourth basalt flows exposed in the upper 50 m of the crater wall (Fig. 1b). Six additional samples of basalt (CF-1 to CF-6 in the Appendix), one each from the six basalt flows exposed in the Lonar area, were also collected by one of us (S. Ghosh) for the present study. The four bottom flows were sampled from the crater wall exposed along the main incision at the northeast crater rim (Fig. 1b). In general, all basalt flows have a common mineralogy and texture, with the exception of some minor petrographic differences in the abundance of plagioclase phenocrysts, glass, and opaques (Ghosh and Bhaduri 2003). The basalts are porphyritic with phenocrysts of plagioclase and rare olivine that are set in a groundmass of plagioclase, augite, pigeonite, titanomagnetite, palagonite and other secondary minerals like calcite, zeolite, chlorite, serpentine, and chlorophaeite.

The present populations of basalts at Lonar are mainly vesicular, porphyritic basalts containing euhedral prismatic megacrystic plagioclase phenocrysts and porphyries of prismatic plagioclase of smaller dimension (e.g., Fig. 2). Plagioclase phenocrysts with elongated rod-like crystals also occur either as single or aggregated crystals. Some megacrystic plagioclase crystals show compositional zoning and contain relicts of subhedral prismatic plagioclase core. The plagioclase laths form triangular and polygonal interstices that are usually occupied by anhedral clinopyroxene. Euhedral or subhedral, square and rectangular-shaped titano-magnetite in the matrix sometimes contain inclusions of subhedral prismatic plagioclase laths. Opaque minerals also occur as smaller, square-shaped grains disseminated in the matrix. The interstitial spaces between the plagioclase grains are, in some cases, occupied by brown-colored and partially devitrified glass. These interstitial glasses comprise about 1 vol% and show color compositional zoning (which could be an alteration effect). Large interstitial glass patches are rare and usually occur in areas dominated by plagioclase megacrysts.

In thin section, none of our target-basalt samples shows obvious evidence of shock metamorphism—except, in a few cases, the development of well-spaced fractures oblique to the length of plagioclase megacrysts. The groundmass plagioclase laths, as well as the titano-magnetite do not show any fracturing or other deformational features. These samples likely belong to the class I shock-metamorphosed basalt as described by Kieffer et al. (1976).

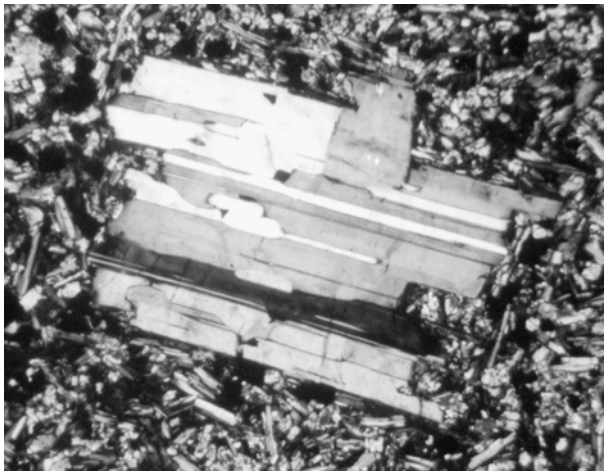

Fig. 2. Porphyritic unshocked basalt from location L-9 the crater rim, showing a twinned plagioclase phenocryst. Width of image ~120 μm, crossed polarizers.

Morphology and Petrography of Impact Glasses

Impact glasses collected from around Lonar Crater can be classified into two broad groups depending on their occurrence: 1) those occurring outside the crater rim within the ejecta blanket, and 2) those occurring inside of the crater rim and around Lonar Lake (Fig. 1b). Some morphological differences exist between these two groups.

Glasses from Outside the Crater Rim

The impact glasses collected from outside the crater rim can further be classified into the following four (a–d) categories according to their size and morphology:

Type “a” glasses, which are mm-size, in situ impact spherules, were recovered from trenches dug through the ejecta blankets to the southeast and western portions of the crater (Sengupta et al. 1997). The glasses were encountered about 5 cm below the alluvium surface in the spherule-rich ejecta horizon. They are characteristically black, have vitreous luster and a highly vesicular surface and a variety of geometric shapes including rod, ellipsoidal, and tear-drop shapes (Fig. 3a). The sizes of the spherules in our population range from 7.4 × 2.8 mm to 2 × 1.5 mm. Secondary infillings of quartz are sometimes found in the vesicles. Nayak (1972) also reported spherules of comparable dimension and morphology from the eastern and western sides of the crater rim, from the upper layer of ejecta-rich soil. Fredriksson et al. (1973) described the microscopic character of these spherules, which they retrieved from a trench dug to the east of the crater. In their description, these spherules were brown in color, although some colorless and darker brown schlieren and partly melted mineral inclusions were present. Flow banding was also reported.

Type “a” glasses exhibit “splash forms” due to their transport and solidification in air subsequent to the impact.

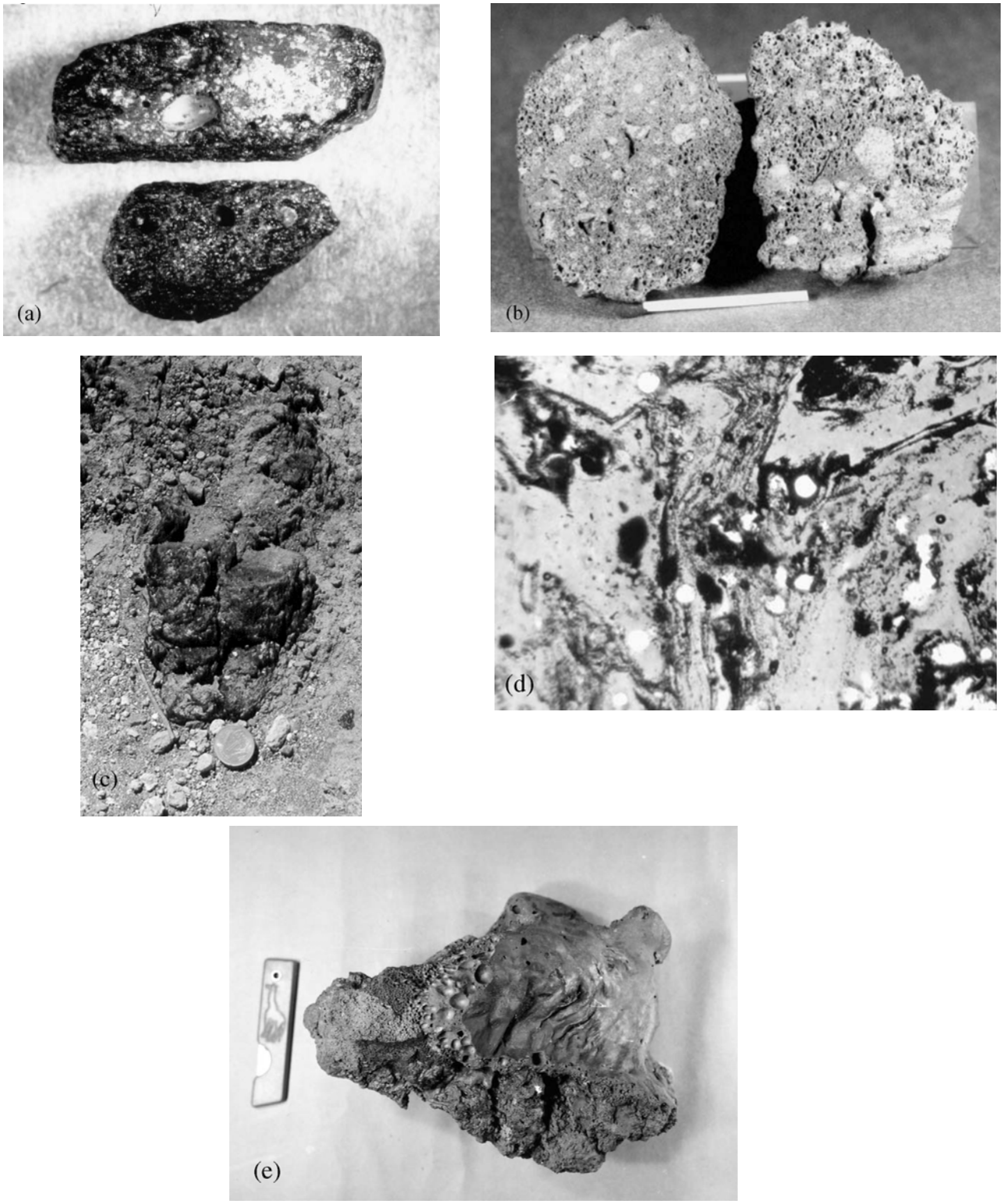

Fig. 3. Impact glass and melt rocks from outside the crater rim: a) two splash-form impact glasses of type “a” recovered from the ejecta blanket, a few cm below the present surface, at location D-1 in Fig. 1b; width of image = 7 mm; b) type “b” impactite in cross-section, showing angular basalt fragments; length of match = 2.9 cm; c) occurrence of type “c” impact melt rock in the ejecta blanket outside the southeastern part of the crater rim; diameter of coin = 2.5 cm; d) flow texture in type “c” impact melt rock defined by alternate wide layers of silicate melt and thin magnetite-rich layer. Note the development of microlites between the layers radiating from common centers; crossed polarizers; width of image = ~120 μm; e) type “d” glass-rich vesicular impactite, showing smooth flow-textured surface and vesicular interior; long dimension of sample = ~16 cm.

Thermoluminescence measurements on them (Sengupta 1986) indicate that the TL sensitivity of the glasses is the lowest compared to any other glasses found in and around the crater.

Type "b" glasses, which are not very common, occur around the crater rim within the ejecta blanket and include specimens up to about 5 cm in size (Fig. 3b). These weathered samples are black, have vitreous luster, and are highly vesicular. Angular, mm-size fragments of basalt are dispersed throughout the glasses. Under the microscope, these glasses are not very transparent and heterogeneous, and they contain abundant inclusions of fragmented plagioclase and anhedral clinopyroxene without any preferred orientation. Angular basalt pieces of mm to sub-mm size are also present in the glass matrix. Very small magnetite grains dispersed throughout the mesostasis often cluster into large rectangular or irregular aggregates.

Type "c" glasses represent some melt rock bombs and constitute about 1 vol% of the total ejecta blanket. They mainly occur within the ejecta cover at the eastern flank of the crater at a distance of about 150 m from the crater rim and at a depth of ~1 m from the surface (Ghosh and Bhaduri 2003). These bombs vary in size from ≤1 cm to as large as ~30 cm across, have mottled brown to pitch black color, are highly vesicular, show vitreous luster on freshly broken surfaces, and display flow structure in hand specimen. Under the microscope, these melt rocks show clasts of unmelted breccia containing fragments of pyroxene, glass, and shocked plagioclase.

The impact melt samples belonging to the type "c" category were also recovered in the present study from ~47 cm-deep pit on ejecta blanket close to the southeastern part of the crater rim (Fig. 1b). Some fragments of these impact melt rocks were also found adjacent to the exposure and on the southern slope of the crater close to the crater rim; these may not be in situ, probably due to erosion. These samples are ellipsoidal in shape and have sizes in the centimeter range (Fig. 3c). Our largest bomb has a size of ~9 × 14 × 11 cm. In hand specimen, these impact melt rocks appear black in color, are vesicular, and show ropy or flow structures on the surface. Under the microscope, these glasses appear brown in color and also show flow structures (Fig. 3d). The brownish glasses usually contain unmelted fragments of basalt of various degree of shock deformation, fragments of clinopyroxene and plagioclase, and crystals of magnetite.

Type "d" glasses are glasses that show evidence for having been transported and are found on the outer slope of the ejecta blanket, southwest of Little Lonar and south of Lonar Crater (Fig. 1b). These impactites (Fig. 3e) are much larger compared to the other types and appear similar to those found inside the crater rim (see below). The largest sample, occurring adjacent to Little Lonar, has a dimension of 20 × 20 × 7 cm. These specimens are irregularly shaped and flattened, black in color, show vitreous luster on freshly broken surfaces, and are highly vesicular. One side of the specimens is usually smooth and shows flow structure, with the development of wrinkles perpendicular to the direction of flow (Fig. 3e). The other side of a sample is typically flat. Calcareous encrustation occurs in cases on the surface and in cases present in vesicles. Type "d" glasses are petrographically very similar to the ellipsoidal glasses of type "b." Under the microscope, they are opaque, heterogeneous, and highly vesicular glass containing fragments of plagioclase crystals, anhedral to subhedral clinopyroxene, relict fragments of basalt, and crystals of magnetite. The fragmental plagioclase and clinopyroxene show no preferred orientation or any evidence of shock metamorphism.

Impactites and Impact Glasses from within the Crater

Many of the vesicular impactites that occur inside the crater rim (and also some from outside) have been cut into bricks that have been used in temple constructions in the crater (dating from the 6th century onwards) (Figs. 4a–4c); this use of impactites for religious buildings provides an interesting analogy with the use of suevite from the Ries crater (Germany) in the construction of St. George's church in Nördlingen. The impactites (melt rocks) and impact glasses occurring inside the crater can be classified into two groups (e and f) based on their morphology and petrography.

Type "e" impactites, recovered from north of the Goddess Durga Temple at the western side of the lake (next to location 6 in Fig. 1b) are found underneath soil at a depth of about 1 m below the surface. It was partly exposed along a dried-up stream. The largest sample is roughly tabular having a size of about 12 × 7.5 × 4 cm (Fig. 4d). In hand specimen, this sample is black in color and has a highly irregular surface with less frequent vesicles. Voids are rather common on the surface. It has a dull appearance but shows a vitreous luster on the surface in the interior of vesicles or on freshly broken surfaces. Infillings of quartz usually occupy these voids.

Microscopic observations of these glasses show porphyritic basalt with euhedral prismatic plagioclase phenocrysts, as observed in the Deccan basalt target-rocks. There are some fractures in the plagioclase phenocrysts as well as in the plagioclase laths in the groundmass. Opaque glass is present in the interstitial spaces between plagioclase laths (Fig. 4e). Euhedral or subhedral titano-magnetite grains have also been observed in these samples and show a high degree of fragmentation. These minute, angular and opaque fragments are distributed throughout the sample without any preferred orientation.

Type "f" glasses are black on freshly broken surfaces, highly vesicular, and have relatively low specific gravity. The glasses show vitreous luster, particularly on interior vesicle surfaces. In many cases one side of the sample is flat, while the others show flow features and have variable morphology (Fig. 4f). One sample, collected from a location near the

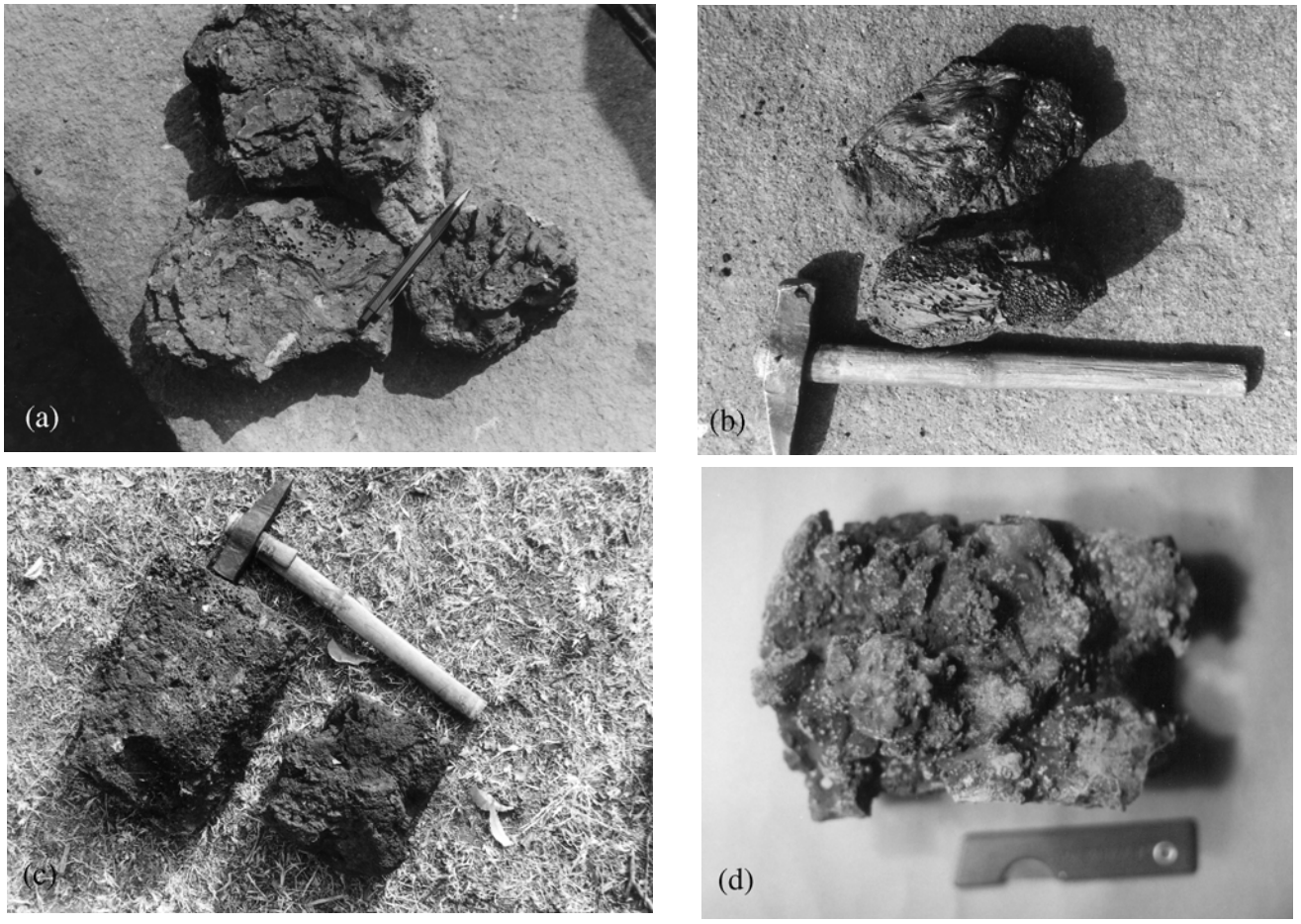

Fig. 4. Glass-bearing impactites from inside the crater rim: a) three pieces of highly vesicular glass-bearing impactite (location 6); flow texture well recognizable; length of pen = 13 cm; b) two vesicular impactite specimens with well-preserved flow texture on the surface, showing extended vesicles (location 26; hammer = 40 cm long); c) vesicular impactite cut into bricks that have been used in temple construction within the crater; location 8; hammer = 40 cm long; d) hand specimen of a type "e" impactite (shocked basalt) collected near the western edge of Lonar Lake; length of plastic scale bar = 7.3 cm.

Goddess Durga Temple to the west of the lake (loc. 6, Fig. 1b), has an ellipsoidal shape. One side of the sample is typically vesicle-rich and flat, while the other side is hemispherical in shape and shows flow structures (Fig. 4f). Another sample, collected from the site of a broken ancient temple near location 6 is irregular in shape with a nearly flat base, grayish black in color on a fresh surface, and shows good flow structure on the upper side of the sample (Fig. 4c). These samples are in many cases very similar to the old earthen bricks used by ancient people for construction of temples, and can easily be confused with these.

These large pieces of glass are petrographically very similar to the type "b" and "d" glasses occurring outside the crater rim in the ejecta blanket. In cross-section, these impactites show a few subrounded to subangular basalt phenocrysts up to about 5 mm in size in highly vesicular mesostasis (Fig. 4g).

In summary, the impact glasses and melt rocks recovered from around and within the Lonar Crater can be classified into two fundamental petrographic classes. Class I glasses include type "a" and "c" glasses, which are black and brown-colored transparent glasses occurring outside the crater rim within the ejecta blanket and which show schlieren and flow structures under the microscope. The presence of unmelted fragments of basalt, fragments of clinopyroxene and plagioclase, and crystals of magnetite are additional features. Class II glasses include type "b," "d," and "f" glasses, which are opaque under the microscope, containing abundant inclusions of unshocked fragments of plagioclase and clinopyroxene.

Geochemistry

A total of 19 basalt, 17 impact melt rock, and 7 impact glass samples were analyzed for their major and trace element composition (Tables 1–3). Average compositions and standard deviations for our data, together with literature data for the major element and selected trace element contents of averages of previous data for Deccan basalts, are reported in

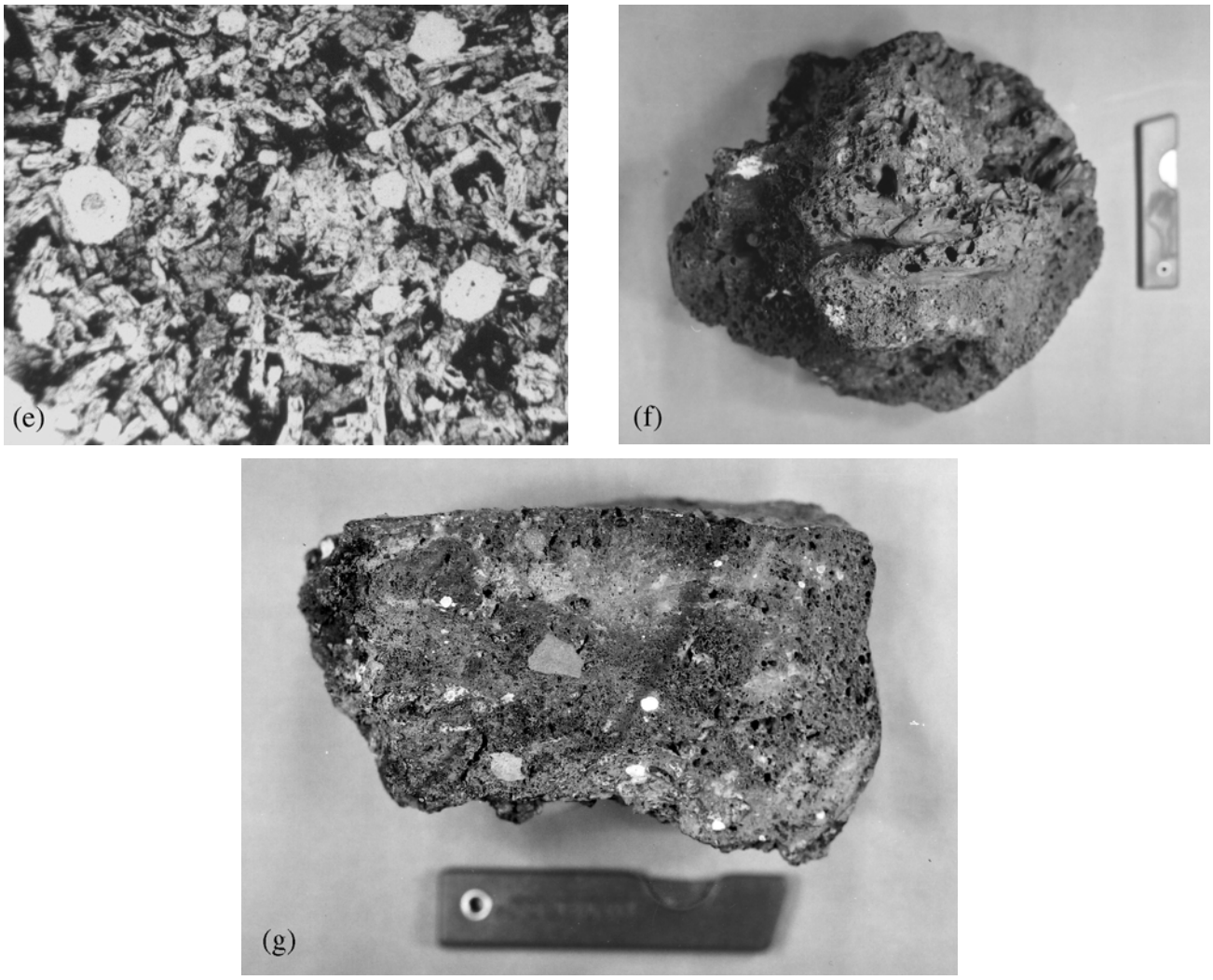

Fig. 4. *Continued.* Glass-bearing impactites from inside the crater rim: e) microphotograph of type "e" impactite showing small patches of non-transparent interstitial melt between plagioclase laths; crossed polarizers; width of image = 120 μm; f) type "f" impact melt, showing a smooth upper surface; length of plastic scale bar = 7.3 cm; sample collected at the western side of Lonar lake; g) cut surface of one of the large impactite specimens found at the inner crater rim, showing sub-angular basalt clasts and a vesicular, glass-rich matrix of different colors, ranging from light tan to dark gray; sample from location 8; plastic scale bar = 7.3 cm long.

Table 4. The range of compositions of the Deccan basalts at Lonar is quite limited, as can be seen from the individual values given in Table 1. This is the case for both, major and trace elements, although a few elements, such as the alkali elements Cr and Ba, and some of the volatile elements, show wider compositional ranges than the other elements. The comparison with "average Deccan Trap" basalts (Table 4) indicates a few minor differences. The silica contents of the Lonar basalts are slightly lower, and the Ca and Na contents are slightly higher than the literature values for average Deccan basalts. On the other hand, our data agree well with other published data on Lonar Deccan basalts (Kieffer et al. 1976; Widdowson et al. 2000; Ghosh and Bhaduri 2003).

A general comparison of the average major element composition of target basalt and impact melt rocks shows that their compositions are closely related, but notable differences relate to the abundances of Na, K, and P (Fig. 5). Six of the impact-melt rock samples (L-27A, L-36, L-37X, L-44, L-4, and L-6B) of class II have elevated levels of K relative to Na, but their Na contents are relatively high compared to those of the target basalts. Only samples L-37X and L-6B have substantially lower Na contents relative to K, similar to the samples reported from melt rocks at Brent (Grieve 1978) and Ames (Koeberl et al. 1997) impact structures. Moderately enriched values of K, compared to Na, may be the result of vaporization or post-impact hydrothermal processes, as discussed in detail by Puura et al. (2004). In our samples, indications of a post-impact hydrothermal influence are ambiguous because the high Cr and Ni abundances in all analyzed samples are associated with rather low levels of As, elevated values of which might indicate hydrothermal activity. However, this could be because any impact-induced

Table 1. Chemical composition of target basalt samples (Deccan basalts) from the Lonar crater, India.[a]

	CF-1	CF-2	CF-3	CF-4	CF-5	CF-6	L-9	L-10	L-11	L-14	L-15	L-16	L-21	L-34	L-35	L-38	L-41	L-42	L-43
SiO_2	49.11	48.77	45.27	46.30	47.39	46.74	47.57	48.82	48.96	46.48	49.03	48.54	48.84	47.22	50.02	45.58	47.84	46.89	49.14
TiO_2	2.41	2.40	2.41	2.67	2.09	1.95	2.10	1.63	2.40	2.40	2.33	2.28	2.38	2.44	1.91	2.59	2.20	2.17	2.22
Al_2O_3	12.81	13.06	15.11	12.87	13.14	13.39	12.89	12.68	12.93	12.55	12.65	13.11	12.87	13.08	12.76	12.29	12.47	12.54	13.04
Fe_2O_3	15.99	15.78	15.94	16.46	14.74	15.08	15.83	14.87	15.29	16.04	15.94	15.60	16.18	16.39	15.40	17.14	15.73	16.41	15.45
MnO	0.19	0.18	0.25	0.21	0.17	0.19	0.20	0.17	0.17	0.22	0.17	0.13	0.13	0.30	0.18	0.19	0.19	0.21	0.20
MgO	5.65	5.87	6.00	6.26	6.78	7.20	6.39	6.26	5.63	6.41	5.53	6.02	5.54	6.21	5.54	6.27	5.94	6.18	5.56
CaO	9.44	9.34	10.1	10.3	9.97	10.7	10.2	9.96	9.32	10.3	9.40	9.60	9.36	10.19	9.78	9.79	10.1	10.1	9.53
Na_2O	3.20	2.81	2.82	3.10	2.31	3.24	3.09	2.71	2.96	3.03	2.79	2.94	2.87	3.05	3.15	3.04	3.24	3.47	3.11
K_2O	0.41	0.49	0.20	0.17	0.18	0.17	0.23	0.33	0.44	0.22	0.73	0.53	0.70	0.32	0.58	0.49	0.39	0.37	0.28
P_2O_5	0.24	0.25	0.22	0.22	0.21	0.20	0.23	0.25	0.26	0.45	0.37	0.28	0.25	0.24	0.46	0.22	0.25	0.24	0.24
LOI	0.52	0.95	1.56	1.40	2.54	0.28	0.49	1.36	0.80	1.20	1.11	0.68	0.72	0.74	0.49	1.81	0.83	0.15	1.34
Total	99.97	99.90	99.86	99.92	99.52	99.11	99.17	99.04	99.16	99.26	100.05	99.71	99.84	100.18	100.27	99.41	99.14	98.70	100.11
Sc (ppm)	36.5	34.4	35.8	36.1	34.3	37.6	36.2	35.7	34.7	36.9	36.0	35.9	34.7	37.7	35.7	37.8	35.7	36.7	36.0
V	531	740	480	376	599	463	572	399	690	440	401	639	607	544	475	376	587	599	359
Cr	134	219	137	77.8	307	129	83.8	223	98.4	85.0	44.0	88.0	150	122	90.6	34.7	65.1	38.3	96.9
Co	48.9	46.3	48.2	48.7	50.0	51.6	49.0	49.1	46.1	49.0	47.8	47.3	46.3	50.3	47.1	51.1	46.4	47.5	47.7
Ni	73	147	94	63	206	105	81	150	64	61	52	69	92	110	49	58	84	54	102
Cu	209	269	222	223	209	224	205	198	228	216	199	211	224	233	223	194	214	236	233
Zn	126	249	121	140	124	125	125	105	122	121	118	126	124	124	125	121	131	133	127
As	0.49	0.48	0.18	0.22	<0.78	0.42	1.05	0.34	0.83	0.54	0.78	1.85	0.51	0.66	0.41	0.56	0.49	0.39	0.15
Br	0.2	0.3	0.2	<0.8	0.4	0.5	0.1	0.2	0.4	<0.6	<0.5	<0.4	0.2	0.3	0.2	<1.0	0.2	<1.2	<1.00
Rb	22.4	9.06	2.7	2.7	5.8	<0.5	3.1	1.7	20.1	1.74	22.0	18.5	14.2	5.1	7.4	21.7	19.3	3.5	4.7
Sr	251	218	231	226	201	200	227	212	249	227	219	251	252	228	230	218	250	228	226
Y	25	28	28	30	26	30	29	22	34	36	36	31	31	31	31	28	22	36	33
Zr	214	181	175	159	127	124	153	139	190	166	170	216	190	184	168	168	174	151	158
Nb	12	11	10	11	9	8	11	8	13	11	10	13	13	11	11	10	12	11	10
Sb	0.08	0.11	0.06	0.06	0.06	0.05	0.08	0.05	0.06	0.10	0.11	0.12	0.07	0.05	0.04	0.04	0.10	0.05	0.04
Cs	0.34	0.29	0.07	0.07	0.14	0.11	0.17	0.03	0.48	0.05	0.31	0.57	0.31	0.08	0.04	0.04	0.24	0.23	0.31
Ba	145	106	96	86	53	64	76	61	144	92	98	154	156	110	102	118	147	107	114
La	17.2	13.5	11.9	12.1	7.8	7.4	12.8	9.6	16.8	13.1	12.8	16.3	16.7	13.8	12.5	13.3	16.6	13.7	12.9
Ce	39.4	30.5	28.1	29.4	19.4	20.7	30.4	22.8	37.5	31.1	31.5	39.0	37.3	31.9	29.9	31.3	38.3	33.0	30.2
Nd	24.4	20.5	18.4	20.6	14.0	13.7	20.9	13.7	22.8	18.2	19.2	22.6	22.3	22.3	19.6	21.7	24.9	23.9	19.3
Sm	6.36	5.99	5.18	5.74	4.39	4.43	5.63	4.45	6.36	5.60	5.40	6.09	5.79	6.19	5.18	5.86	6.35	5.89	5.99
Eu	2.30	2.09	2.05	2.07	1.60	1.75	2.17	1.76	2.13	2.18	2.14	2.16	2.12	2.22	2.01	2.17	2.06	2.14	2.04
Gd	5.65	6.24	5.48	5.60	4.68	4.98	5.54	5.10	7.05	6.11	5.85	5.94	6.23	6.31	6.51	6.7	7.6	7.23	7.14
Tb	1.03	1.14	0.93	1.06	0.80	0.87	1.07	0.91	1.24	1.11	0.97	0.90	1.07	1.17	1.03	1.13	1.18	1.29	1.15
Tm	0.54	0.51	0.46	0.51	0.33	0.39	0.46	0.36	0.52	0.50	0.48	0.42	0.44	0.56	0.48	0.5	0.56	0.51	0.49
Yb	2.95	2.98	2.82	2.79	2.29	2.84	2.70	2.40	2.80	2.99	2.93	2.84	2.91	3.12	2.86	2.88	2.88	3.27	3.02
Lu	0.44	0.43	0.42	0.40	0.33	0.44	0.40	0.35	0.43	0.45	0.40	0.43	0.43	0.47	0.43	0.43	0.45	0.47	0.45
Hf	4.85	4.09	3.85	4.05	3.05	3.27	3.98	3.23	3.23	4.13	4.13	4.67	4.77	4.26	4.14	4.23	4.63	4.20	3.87
Ta	0.87	0.84	0.60	0.88	0.56	0.60	0.80	0.46	0.46	0.75	0.68	0.93	0.87	0.77	0.57	0.80	0.85	0.92	0.73
W	2.6	<2.4	0.8	<3.5	1.6	0.6	<4.4	<3.5	1.8	<3.6	1.5	<3.5	<5.0	<4.3	2.2	2.7	2.3	1.8	<5.1
Ir (ppb)	<1.8	<2.0	<1	<1.5	<2.6	<3.1	<1.5	<1.5	<1.2	<0.6	<1.2	<1.5	<1.6	<1.5	<1.5	<0.6	<1.0	<0.8	<0.5
Au (ppb)	1.1	3.2	1.0	4.1	3.5	1.8	3.0	2.1	1.5	2.3	3.6	1.1	3.6	1.8	1.2	1.8	3.5	1.7	2.5
Th	2.61	1.92	1.67	1.93	0.86	1.05	1.85	1.25	2.64	1.84	1.78	2.56	2.55	1.93	1.70	1.81	2.49	1.81	1.86
U	0.77	0.51	0.29	0.41	0.28	0.55	0.33	0.48	0.70	0.80	0.60	0.55	0.68	0.60	0.35	0.62	0.74	0.36	1.27

Table 1. *Continued.* Chemical composition of target basalt samples (Deccan basalts) from the Lonar crater, India.[a]

	CF-1	CF-2	CF-3	CF-4	CF-5	CF-6	L-9	L-10	L-11	L-14	L-15	L-16	L-21	L-34	L-35	L-38	L-41	L-42	L-43
K/U	4437	8006	5747	3455	5357	2576	5808	5729	5238	2292	10139	8030	8578	4444	13809	6586	4392	8564	1837
Th/U	3.39	3.76	5.76	4.71	3.07	1.91	5.61	2.60	3.77	2.30	2.97	4.65	3.75	3.22	4.86	2.92	3.36	5.03	1.46
La/Th	6.59	7.03	7.13	6.27	9.07	7.05	6.92	7.65	6.36	7.12	7.19	6.37	6.55	7.15	7.35	7.35	6.67	7.57	6.94
Zr/Hf	44.1	44.3	45.5	39.3	41.6	37.9	38.4	42.9	58.8	40.2	41.2	46.3	39.8	43.2	40.6	39.8	37.7	36.0	40.9
La_N/Yb_N	3.94	3.06	2.85	2.93	2.30	1.76	3.20	2.69	4.05	2.96	2.95	3.88	3.88	2.99	2.95	3.12	3.89	2.83	2.89
Eu/Eu*	1.17	1.04	1.18	1.12	1.08	1.14	1.19	1.13	0.97	1.14	1.16	1.10	1.08	1.09	1.06	1.06	0.91	1.00	0.95

[a]The sample numbers refer to location numbers given in the Appendix and in Fig. 1b. Major element data in wt%; trace element data in ppm, except as noted. All Fe calculated as Fe_2O_3.

Table 2. Chemical composition of impact melt rock and breccia samples from the Lonar crater, India.[a]

	L-22	L-23	L-27A	L-29	L-36	L-37X	L-44	GSI-1	SG-1	SG-2	SG-3	L-4	L-6A	L-6B	L-7	L-8	L-13B
SiO_2 (%)	48.13	50.66	59.34	50.77	57.43	58.13	55.40	51.15	50.35	49.35	50.66	56.04	56.55	–	47.10	51.33	45.73
TiO_2	2.33	2.46	1.60	2.21	1.71	1.43	2.05	2.29	2.08	2.24	2.23	1.79	1.80	–	2.50	1.87	3.13
Al_2O_3	13.38	13.48	11.39	13.57	11.80	11.19	12.78	13.81	13.31	13.36	13.75	12.51	10.71	–	12.93	13.76	13.01
Fe_2O_3	15.87	16.75	11.66	15.25	12.13	11.05	14.16	14.98	14.73	15.20	14.95	12.83	11.25	11.48	16.51	14.04	18.42
MnO	0.19	0.23	0.16	0.24	0.12	0.12	0.19	0.19	0.20	0.19	0.22	0.18	0.18	–	0.21	0.18	0.20
MgO	6.04	5.68	4.16	5.54	4.26	4.48	4.51	5.56	5.44	5.67	5.73	4.52	4.31	–	5.51	6.66	6.98
CaO	10.19	8.15	7.91	9.83	7.63	8.79	7.39	9.40	9.33	9.68	9.68	7.85	8.64	–	8.98	8.87	8.71
Na_2O	2.15	1.25	1.04	1.97	1.11	0.85	1.14	1.93	2.16	2.33	2.06	1.00	0.00	0.77	3.88	1.83	1.43
K_2O	0.55	0.89	1.61	0.71	1.25	1.95	1.58	0.73	0.73	0.57	0.54	1.79	1.86	2.43	0.91	0.78	0.15
P_2O_5	0.23	0.40	1.07	0.30	0.82	1.19	0.87	0.28	0.37	0.25	0.27	1.09	1.13	–	0.32	0.34	0.20
LOI	0.06	0.03	0.02	0.03	0.05	0.11	0.21	0.05	0.21	0.33	0.03	0.11	3.21	–	0.05	0.04	1.37
Total	99.12	99.98	99.96	100.42	98.31	99.29	100.28	100.37	98.91	99.17	100.12	99.71	99.64	–	98.90	99.70	99.33
Sc (ppm)	36.6	38.9	27.6	35.6	27.3	24.4	32.8	33.5	33.7	33.8	33.7	29.7	25.1	26.8	37.8	31.7	41.0
V	506	756	242	552	268	224	410	573	516	575	570	309	–	–	699	360	2249
Cr	105	218	120	101	123	141	144	75.6	148	149	98	135	95	112	121	91.6	547
Co	46.2	54.8	37.1	44.5	38.0	34.5	45.2	41.5	41.8	41.9	41.5	40.2	34.5	37.4	46.9	41.2	58.9
Ni	75	100	67	78	97	67	64	66	88	102	78	98	73	96	86	74	156
Cu	198	167	195	196	191	170	153	209	185	197	201	149	–	–	150	167	228
Zn	134	153	183	137	172	254	163	131	119	129	128	203	221	245	148	131	255
As	<1.04	<0.87	4.01	0.60	0.44	0.29	0.60	<0.89	0.43	6.99	<0.96	0.26	0.88	0.42	<1.4	<0.8	<1.55
Br	<0.9	<0.5	<2.0	<0.8	0.7	0.4	0.3	1.1	0.8	0.9	0.8	1.7	1.9	2.3	2.1	1.9	1.2
Rb	21.4	17.8	35.2	23.3	36.3	36.2	31.4	19.9	19.2	21.3	20.5	35.7	43.6	45.0	14.3	25.4	16.0
Sr	248	171	195	255	180	222	184	264	245	254	252	187	–	–	251	237	137
Y	27	30	27	35	31	16	29	30	27	29	36	24	–	–	27	31	30
Zr	212	151	144	194	149	107	158	222	213	222	94.5	155	131	175	183	182	147
Nb	11	12	10	12	11	8	11	13	11	12	12	10	–	–	12	11	13
Sb	<0.16	0.13	0.15	0.06	0.22	0.11	0.06	<0.13	<0.1	<0.1	<0.1	0.06	0.13	0.11	<0.1	<0.1	0.08
Cs	0.36	0.63	1.05	0.33	1.14	1.07	1.03	0.32	0.26	0.34	0.45	1.02	1.14	1.14	0.46	0.65	0.20
Ba	153	147	152	207	164	157	174	217	163	207	198	176	–	–	167	141	63
La	19.1	12.9	13.7	20.3	13.3	12.4	14.8	19.5	17.2	18.5	18.4	13.2	12.8	12.9	13.6	14.2	8.38
Ce	41.1	30.9	31.3	43.9	30.4	28.5	34.1	43.7	40.4	41.6	40.5	31.8	29.3	31.2	30.3	32.9	21.4
Nd	25.3	21.1	18.3	24.9	17.4	16.5	19.4	27.7	23.9	25.8	27.3	19.7	18.3	20.3	21.5	22.3	16
Sm	6.18	5.70	4.55	6.37	4.82	3.93	5.25	6.09	5.71	6.02	6.28	4.60	4.15	4.42	5.35	4.92	4.36
Eu	2.03	1.87	1.52	2.21	1.56	1.36	1.77	2.04	1.89	1.96	1.86	1.53	1.38	1.41	2.03	1.9	1.52
Gd	6.28	5.27	5.05	5.89	4.67	4.11	5.90	6.5	5.4	6.44	5.53	5.0	4.27	4.88	5.02	5.2	4.83

Table 2. *Continued.* Chemical composition of impact melt rock and breccia samples from the Lonar crater, India.[a]

	L-22	L-23	L-27A	L-29	L-36	L-37X	L-44	GSI-1	SG-1	SG-2	SG-3	L-4	L-6A	L-6B	L-7	L-8	L-13B
Tb	1.14	0.99	0.83	1.05	0.87	0.70	0.89	1.08	0.96	1.00	0.99	0.80	0.64	0.79	0.86	0.83	0.85
Tm	0.50	0.42	0.36	0.53	0.44	0.33	0.45	0.45	0.42	0.44	0.46	0.38	0.32	0.35	0.4	0.45	0.46
Yb	2.79	2.65	2.18	2.89	2.44	2.06	2.49	3.05	2.74	2.91	2.94	2.33	2.02	2.18	2.65	2.66	2.54
Lu	0.41	0.38	0.33	0.43	0.37	0.30	0.37	0.45	0.41	0.42	0.44	0.34	0.31	0.32	0.39	0.39	0.36
Hf	4.54	4.13	3.45	4.75	3.50	3.03	4.01	4.89	4.24	4.56	4.60	3.62	3.39	3.51	4.40	3.93	3.90
Ta	0.74	0.79	0.58	0.81	0.64	0.61	0.73	0.61	0.58	0.68	0.72	0.69	0.52	0.56	0.72	0.53	0.67
W	<4.7	<4.1	3.6	<3.2	3.4	2.1	1.4	<3.1	<4.2	<3.2	0.7	2.0	4.5	2.1	<4.1	1.7	<3.9
Ir (ppb)	<2.0	<4.0	<3.0	<4.0	<2.5	<3.5	<3.0	<1.0	<1.5	<1.1	<1.0	<1.7	<1.3	<1.0	<1.2	<2.0	<1.5
Au (ppb)	1.5	0.9	5.5	1.6	4.7	6.4	2.6	<1.0	<0.9	1.2	<2.0	1.6	4.4	3.3	<1.0	1.6	1.5
Th	2.91	2.24	2.76	2.91	2.29	2.63	3.10	2.87	2.53	2.82	2.88	2.92	2.90	3.09	2.09	2.46	1.20
U	0.73	0.40	0.73	0.44	0.70	0.32	0.47	0.66	0.68	0.38	0.40	0.36	0.41	0.75	0.23	0.48	<0.5
K/U	6278	18541	18378	13446	14880	50779	28013	9217	8946	12500	11250	41434	37803	26999	32970	13541	–
Th/U	3.99	5.60	3.78	6.61	3.27	8.22	6.60	4.35	3.72	7.42	7.20	8.11	7.07	4.12	9.09	5.13	–
La/Th	6.56	5.76	4.96	6.98	5.81	4.71	4.77	6.79	6.80	6.56	6.39	4.52	4.41	4.17	6.51	5.77	6.98
Zr/Hf	46.7	36.6	41.7	40.8	42.6	35.3	39.4	45.3	50.2	48.8	20.5	42.8	38.8	49.8	41.5	46.4	37.6
La_N/Yb_N	4.63	3.29	4.25	4.75	3.68	4.07	4.02	4.32	4.24	4.30	4.23	3.83	4.28	4.00	3.47	3.61	2.23
Eu/Eu*	1.00	1.04	0.97	1.10	1.00	1.03	0.97	0.99	1.04	0.96	0.96	0.97	1.00	0.93	1.20	1.15	1.01

[a]The sample numbers refer to location numbers given in the Appendix and in Fig. 1b. Major element data in wt%; trace element data in ppm, except as noted. All Fe calculated as Fe_2O_3. Blank spaces: no data.

Table 3. Chemical composition of impact glasses (spherules, droplets) from the Lonar crater, India.[a]

	DSG-1/A	DSG-1/B	DSG-1/C	DSG-1/E	DSG-1/F	DSG-1/G	DSG-1/H
Fe_2O_3	16.3	15.6	15.2	13.5	16.9	17.9	16.3
Na_2O	2.43	2.39	2.44	2.21	2.50	2.19	2.42
K_2O	0.49	0.76	0.43	0.48	0.45	0.47	0.33
Sc	38.5	37.3	36.8	36.0	39.9	37.7	38.5
Cr	115	120	105	88.2	118	93	124
Co	49.7	48.6	45.2	47.0	54.7	66.0	52.2
Ni	181	117	91	124	89	178	142
Zn	129	122	117	103	147	101	120
As	0.4	0.4	0.5	0.7	0.8	0.9	0.8
Br	1.5	3.0	0.9	0.9	0.5	0.9	0.7
Rb	14.1	17.1	16.0	11.0	28.6	15.8	14.5
Zr	224	186	213	301	220	187	169
Sb	0.04	0.07	0.04	0.05	0.10	0.05	0.05
Cs	0.31	0.41	0.29	0.56	0.62	0.77	0.74
Ba	142	212	176	165	188	149	181
La	15.9	15.1	15.7	14.5	16	18.9	16.4
Ce	36.9	34	34.6	31.7	37.7	44.1	37.9
Nd	23.7	21.8	23.0	19.8	22.5	25.0	22.0
Sm	5.77	5.72	5.58	4.64	5.98	6.2	5.78
Eu	2.25	2.02	1.91	1.75	2.31	2.33	2.20
Gd	5.87	6.00	6.53	4.80	6.50	5.56	6.13

Table 3. *Continued.* Chemical composition of impact glasses (spherules, droplets) from the Lonar crater, India.[a]

	DSG-1/A	DSG-1/B	DSG-1/C	DSG-1/E	DSG-1/F	DSG-1/G	DSG-1/H
Tb	1.08	1.00	1.07	0.79	1.08	1.03	1.05
Tm	0.51	0.48	0.43	0.45	0.50	0.50	0.44
Yb	3.03	3.02	2.88	2.83	3.04	3.31	3.00
Lu	0.44	0.41	0.41	0.42	0.45	0.47	0.42
Hf	4.45	4.33	4.19	3.98	4.31	5.18	4.52
Ta	0.59	0.71	0.58	0.46	0.70	0.97	0.55
W	2.2	<4.4	3.1	<6.3	2.9	3.5	<5.3
Ir (ppb)	<2.1	<2.3	<3.0	<3.3	<2.1	<4.0	<2.4
Au (ppb)	<2.0	<2.0	1.5	1.9	1.3	<5.0	<3.5
Th	2.42	2.57	2.41	2.13	2.68	2.99	2.54
U	0.37	0.53	0.76	0.46	0.35	0.59	0.78
K/U	11127	11936	4757	8696	10615	6638	3476
Th/U	6.54	4.85	3.17	4.63	7.66	5.07	3.26
La/Th	6.57	5.88	6.51	6.81	5.97	6.32	6.46
Zr/Hf	50.4	42.9	50.9	75.6	50.9	36.1	37.4
La_N/Yb_N	3.55	3.38	3.68	3.46	3.56	3.86	3.69
Eu/Eu*	1.18	1.05	0.97	1.13	1.13	1.21	1.13

[a]The sample numbers refer to location numbers given in the Appendix and in Fig. 1b. Major element data in wt%; trace element data in ppm, except as noted. All Fe calculated as Fe_2O_3.

Table 4. Average chemical composition of target basalts, impact melt rock and breccia, and glass spherule samples from the Lonar crater, India, compared with literature data.[a]

	Basalts		Melt rocks		Glass spherules		Mean	Mean	Mean
	Average	Std. dev.	Average	Std. dev.	Average	Std. dev.	W (2000)	G+B (2003)	S+B (1958)
SiO_2	47.82	1.35	52.38	4.18	–	–	48.54	50.55	50.56
TiO_2	2.26	0.25	2.11	–	–	–	2.59	2.52	2.78
Al_2O_3	12.96	0.59	12.80	–	–	–	13.69	13.52	12.79
Fe_2O_3	15.80	0.59	14.19	–	15.94	1.39	15.09	11.40	15.64
MnO	0.19	0.04	0.19	–	–	–	0.22	0.19	n.d.
MgO	6.07	0.45	5.32	–	–	–	6.27	7.64	5.40
CaO	9.85	0.39	8.81	0.85	–	–	10.73	10.14	10.29
Na_2O	3.00	0.25	1.58	0.86	2.37	0.12	2.34	1.70	2.55
K_2O	0.38	0.17	1.12	0.64	0.49	0.13	0.27	0.24	0.59
P_2O_5	0.27	0.08	0.57	0.38	–	–	0.23	0.21	n.d.
LOI	1.00	0.58	0.37	0.83	–	–	n.d.	2.74	n.d.
Total	99.60	–	99.44	–	–	–	99.97	100.85	100.60
Sc	36.0	1.0	32.4	4.9	37.8	1.3	–	–	–
V	520	113	587	488	–	–	361	–	–
Cr	117	69	148	108	109	14	106	–	–
Co	48.3	1.6	42.7	6.5	51.9	7.0	51	–	–
Ni	90	41	86	22	132	37	86	–	–

Table 4. *Continued.* Average chemical composition of target basalts, impact melt rock and breccia, and glass spherule samples from the Lonar crater, India, compared with literature data.[a]

	Basalts		Melt rocks		Glass spherules		Mean	Mean	Mean
	Average	Std. dev.	Average	Std. dev.	Average	Std. dev.	W (2000)	G+B (2003)	S+B (1958)
Cu	219	17	184	23	–	–	226	–	–
Zn	131	29	171	47	120	16	107	–	–
As	0.58	0.39	1.44	2.12	0.6	0.2	–	–	–
Br	0.3	0.1	1.2	0.7	1.2	0.9	–	–	–
Rb	10.3	8.1	27.2	9.8	16.7	5.6	9.2	–	–
Sr	229	16	219	40	–	–	227	–	–
Y	30	4	29	5	–	–	36	–	–
Zr	169	25	167	38	214	43	149	–	–
Nb	11	1	11	1	–	–	11	–	–
Sb	0.07	0.03	0.11	0.05	0.06	0.02	–	–	–
Cs	0.20	0.16	0.68	0.37	0.53	0.20	–	–	–
Ba	107	31	166	37	173	24	86	–	–
La	13.2	2.8	15.0	3.2	16.1	1.4	–	–	–
Ce	31.1	5.8	34.3	6.4	36.7	4.0	–	–	–
Nd	20.2	3.4	21.5	3.7	22.5	1.6	–	–	–
Sm	5.62	0.64	5.22	0.81	5.67	0.50	–	–	–
Eu	2.06	0.18	1.76	0.27	2.11	0.22	–	–	–
Gd	6.10	0.80	5.31	0.71	5.91	0.60	–	–	–
Tb	1.06	0.13	0.90	0.13	1.01	0.10	–	–	–
Tm	0.47	0.06	0.42	0.06	0.47	0.03	–	–	–
Yb	2.86	0.22	2.56	0.32	3.02	0.15	–	–	–
Lu	0.42	0.04	0.38	0.05	0.43	0.02	–	–	–
Hf	4.03	0.53	4.03	0.55	4.42	0.38	–	–	–
Ta	0.73	0.15	0.66	0.09	0.65	0.16	–	–	–
W	1.8	0.7	2.4	1.2	2.93	0.54	–	–	–
Ir (ppb)	<1	–	<2	–	<3	–	–	–	–
Au (ppb)	2.3	1.0	2.8	1.8	1.6	0.3	–	–	–
Th	1.90	0.51	2.62	0.47	2.5	0.3	–	–	–
U	0.57	0.24	0.51	0.17	0.5	0.2	–	–	–
K/U	6054	2960	21561	13270	8178	3297	–	–	–
Th/U	3.64	1.21	5.89	1.88	5.02	1.63	–	–	–
La/Th	7.07	0.63	5.79	1.00	6.36	0.33	–	–	–
Zr/Hf	42.0	4.9	41.5	7.0	49.2	13.3	–	–	–
La_N/Yb_N	3.11	0.59	3.95	0.59	3.60	0.16	–	–	–
Eu/Eu*	1.08	0.08	1.02	0.07	1.12	0.08	–	–	–

[a]The sample numbers refer to location numbers given in the Appendix and in Fig. 1b. Major element data in wt%; trace element data in ppm, except as noted. All Fe calculated as Fe_2O_3; n.d. or blank spaces: no data. Mean W (2000) = average composition of 264 basalt samples from Ambenali, southwest Deccan Wai Subgroup, from Widdowson et al. (2000); Mean G+B (2003) = mean composition of 7 basalt samples collected within or near the Lonar crater; Ghosh and Bhaduri (2003); Mean S+P (1958) = average composition of Deccan basalts, Sukheswala and Poldervaart (1958).

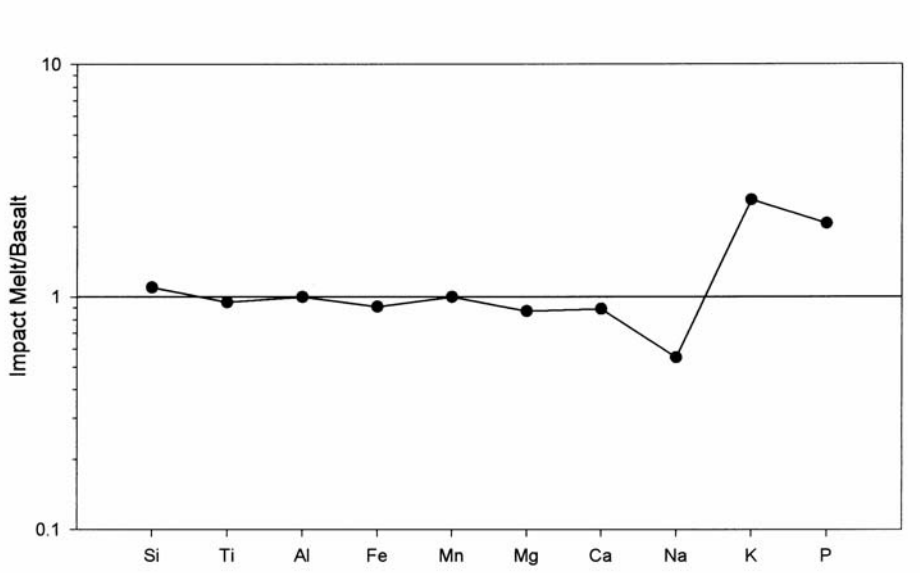

Fig. 5. Comparison of major element compositions of average impact melt rock and target basalt compositions (our data; Table 4).

hydrothermal activity in Lonar Crater, as discussed by Hagerty and Newsom (2003), may have been limited to the crater floor/crater breccia fill, and the samples studied in our work were all collected from near the crater rim, where no such activity would be expected. The slight elevations in the contents of As, Zn, Sb, and Br in the impactites compared to the target basalts (Table 4) could, instead, indicate limited local weathering. However, generally very low LOI values of all samples (even in the melt rocks) indicates little or no influence of carbonates or organic matter, or alteration and the presence of iron and aluminum sesquioxides.

Figure 6 shows data for Lonar impact melt rocks and target rock basalts plotted on various discrimination diagrams, which can be used to classify the basalts and the impactites derived from them. The Zr versus Zr/Y discrimination diagram of Pearce and Norry (1979) shows that the basalts belong to the "within-plate" type (Fig. 6a), while the Cr versus Ti plot (Fig. 6b) and the Ti-Zr-Sr triangular discrimination diagram after Pearce and Cann (1973) show the affiliation to low-K tholeiitic compositions (Fig. 6c). The target rock basalts, though, show a wide variation in Cr from ~30 to 300 ppm, while the impact melt rocks show relatively more limited Cr contents between ~75 and 200 ppm, except for one sample (L-13B) that contains about 550 ppm Cr.

Another set of classification diagrams for Lonar basalts is shown in Fig. 7 (after Floyd and Winchester [1978] and Irvine and Baragar [1971]). The Nb/Y versus Zr/TiO_2 plot confirms the classification of Lonar basalt as a subalkaline basalt (Fig. 7a), while the SiO_2 versus $Na_2O + K_2O$ discrimination plot indicates a compositional spread between alkaline and mostly subalkaline basalt (Fig. 7b). In this diagram, the target rock basalts show very restricted SiO_2 content between about 45 and 50 wt%, while the impact melt rocks show more variation between about 47 and 60 wt%. In an AFM discrimination diagram (after Irvine and Baragar 1971), the Lonar target rock basalt data confirm their tholeiite classification. In summary, the Lonar basalts are classified as relatively low-K tholeiitic within-plate basalts, with a slight Fe and Ca enrichment and a Mg and Al depletion compared to "average" tholeiites (cf. Irvine and Baragar 1971).

Chondrite-normalized rare earth element (REE) abundance plots (Fig. 8) show comparable trends for all samples. No distinct evidence for any variation or fractionation between the basalts and the impactites is seen. Generally, Eu anomalies range from absent (values of Eu/Eu* near 1.0) to very slightly positive (on the order of Eu/Eu* of 1.1). This similarity in the REE patterns indicates little fractionation between the target basalt and the melt rocks and impact glasses. Also, the absence of any noticeable Ce anomalies indicates the absence of extensive alteration and weathering effects for the melt rocks and glasses.

The search for a meteoritic component remains inconclusive. In agreement with earlier work by Morgan (1978), who analyzed the contents of siderophile elements in four Lonar impact glasses and two target basalts and did not find any significant extraterrestrial component, we also note the absence of any siderophile element anomaly in our data. All our Ir values are below the detection limit (depending on sample size and counting statistics on the order of 1 to 3 ppb); this is not surprising because Morgan (1978), using radiochemical neutron activation analysis (which yields better detection limits than our analyses), found Ir values of 5 to 26 ppt in the impact glasses and 4–6 ppt in the target basalts. Assuming a chondritic projectile would, thus, yield an extremely low percentage of extraterrestrial contamination (well below 0.1 percent).

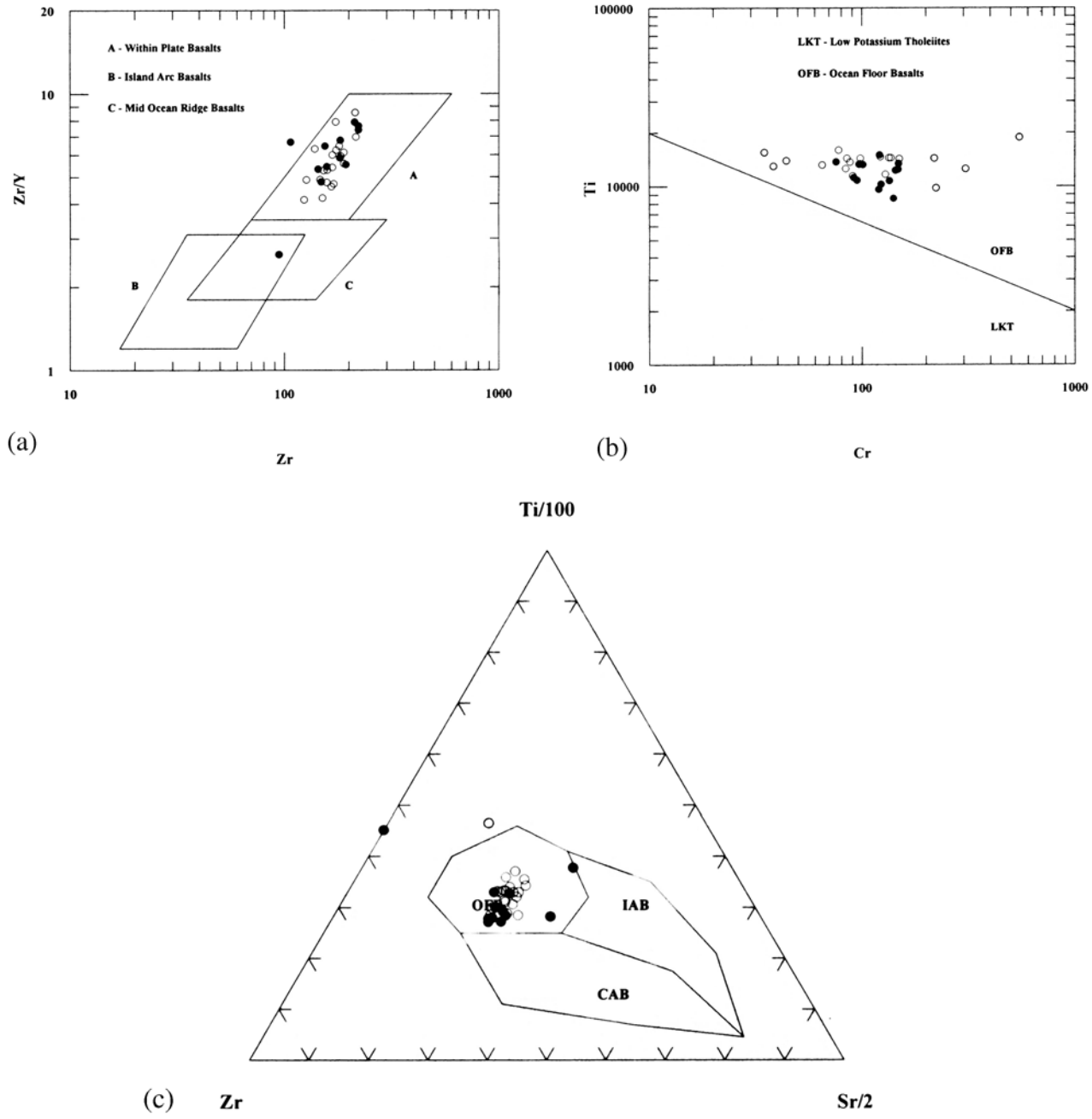

Fig. 6. Data for Lonar impact melt rocks and target basalts plotted on various discrimination diagrams used to classify the basalts and the impactites derived from them. The open and closed circles in this and all subsequent figures represent data for target basalt and impact melt rocks, respectively: a) the Zr/Y-Zr discrimination diagram of Pearce and Norry (1979); b) the Ti-Cr discrimination plot; c) the Ti-Zr-Sr discrimination diagram, both after Pearce and Cann (1973). All contents in ppm.

Alternatively, a crater the size of Lonar is not likely to be the result of a stony meteorite impact anyway, and the projectile could very well have been an Ir-poor iron meteorite.

More recently, Crockett and Paul (2004) analyzed the contents of Ir and other platinum-group elements in a suite of 18 Deccan mafic rocks including 14 basalts and four dolerite dykes from seven different localities in the Maharashtra region of the western parts of the Deccan volcanic province. Based on the distribution of Ir values, these authors distinguished two subsets of samples: one includes 14 samples with average Ir concentration of 0.024 ppb (24 ppt), and the other, a much smaller group of four samples, averages 0.21 ppb Ir; these two subsets are differentiated by other compositional properties in addition to noble metal contents. Crockett and Paul (2004) suggested that these geochemical features indicate that a relatively high percentage of partial

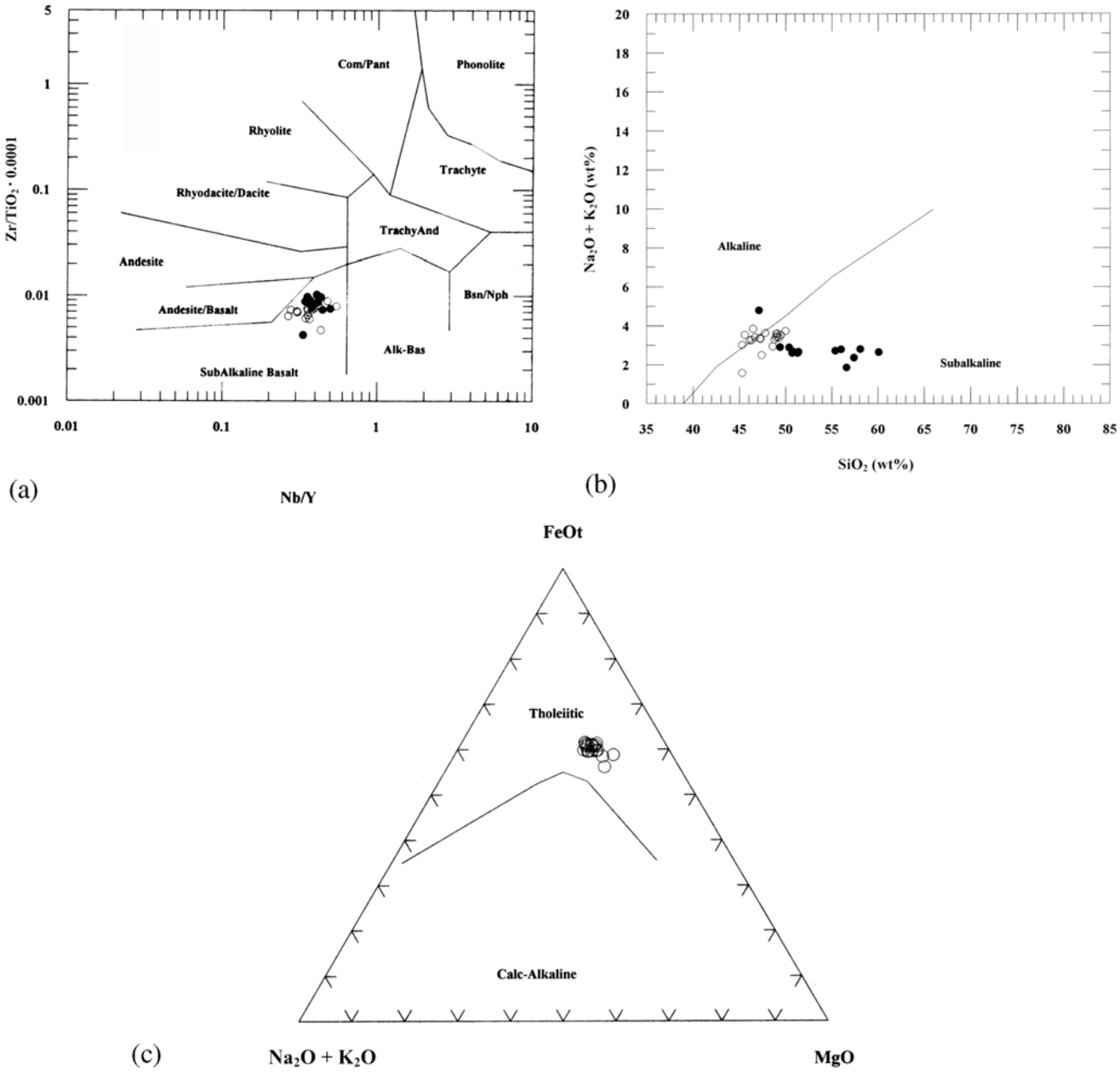

Fig. 7. Classification diagrams for Lonar basalts: a) the Zr/TiO_2-Nb/Y plot, confirming the classification of Lonar basalt as a subalkaline basalt, after Floyd and Winchester (1978); major elements are in wt%, trace elements are in ppm; b) composition of the Lonar basalt shown on a $Na_2O + K_2O$ versus SiO_2 (in wt%) discrimination plot; c) AFM discrimination diagram (after Irvine and Baragar 1971) showing data for Lonar target basalt only.

melting of mantle material is required to generate the Ir-rich magmas. This results in these Deccan rocks having higher concentrations of these elements than other continental flood basalts (Crockett and Paul 2004). Their results also indicate that the Deccan target rocks at Lonar can have Ir contents that overlap those measured by Morgan et al. (1976) for Lonar impact glasses, making the identification of a meteoritic component even more difficult.

Kearsley et al. (2004) reported the presence of some small (<10 μm) iron-nickel particles in vesicles of Lonar impact melts, with a wide range of Fe/Ni ratios (0.02–14.4); it is currently not clear whether or not these fragments represent an indigenous component (maybe reduced during impact) or an extraterrestrial contamination. The rather minor enrichments of the siderophile elements Fe, Co, and Ni in the impact glasses compared to the target basalts (with no enrichment at all for the impact melt rocks), however, indicates that even an iron meteorite component has to be well below one percent.

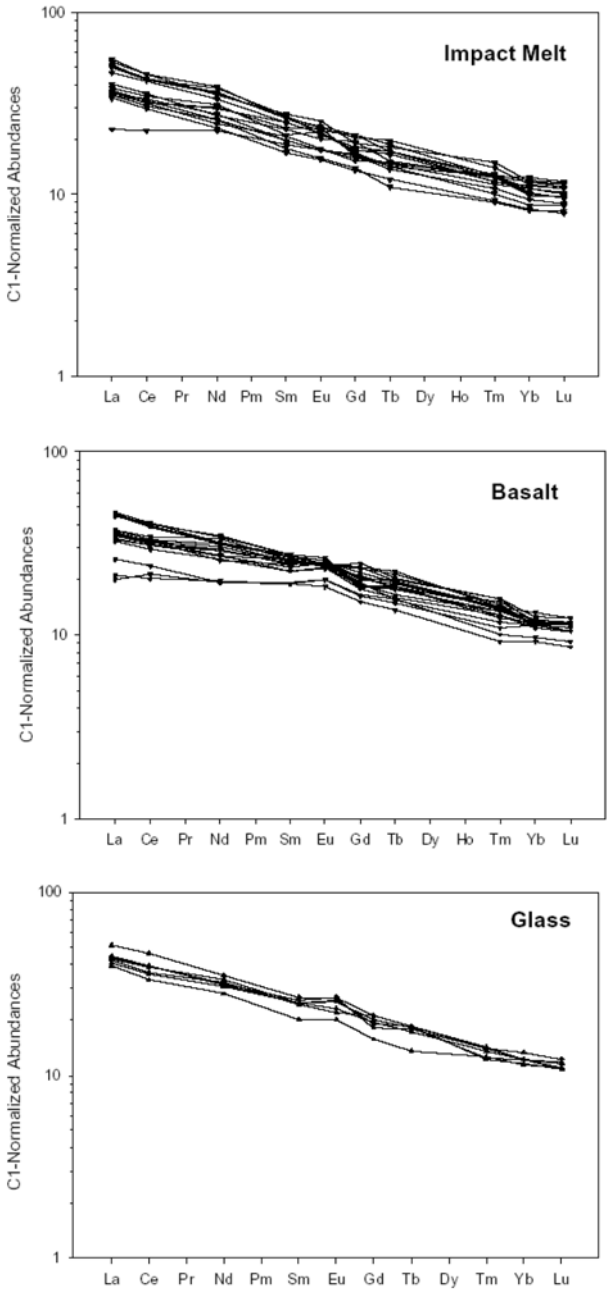

Fig. 8. Chondrite-normalized rare earth element (REE) abundance patterns for Lonar crater impact melt rocks and breccias, target basalts, and glasses, respectively (from top); the normalizing factors are from Taylor and McLennan (1985).

SUMMARY AND CONCLUSIONS

The Lonar impact crater is the only well-preserved terrestrial crater excavated in continental flood basalt and therefore provides a good opportunity to study the characteristics of both terrestrial and martian impacts. The step-like nature of the slope inside the crater rim indicates five flows of ~66–65 Ma Deccan basalt that are exposed by the crater, which have been sampled during the impact.

The mineralogical composition of the post-impact products, such as clasts in melt rocks and impact glasses formed as a result of intense shock metamorphism, at pressures of up to (and possibly exceeding) 60 GPa (see also Fredriksson et al. 1973; Kieffer et al. 1976) confirm the hypervelocity impact origin of Lonar crater.

We found a variety of impact melt rocks and glasses, both inside and outside of the crater rim, which represent a wide range of morphologies and shapes. According to their locations and shapes, these impactites were classified into four morphological groups, which, nevertheless, do not show any significant differences in composition.

The chemical data indicate that there is no significant change between the different basalt flows exposed at Lonar. The basalts can be classified as relatively low-K tholeiitic within-plate basalts, with minor Fe and Ca enrichment and slight Mg and Al depletion compared to “average” tholeiites. The differences between the basalts at Lonar and “average” Deccan basalts are minor and possibly the result of limited sampling at Lonar. The impact melt rocks show some minor differences in the abundances of volatile elements compared to the target basalts, which is probably due to minor post-impact alteration and weathering, but none of the samples analyzed by us from inside or outside the crater rim shows any definite evidence of impact-indicated hydrothermal alteration.

Additionally, the similarity between the chondrite-normalized REE abundances of the impactites (melt rocks and impact glasses) and those of the target basalt indicates that no fractionation or significant alteration occurred during or after the impact process. A search for an extraterrestrial component in the glasses and melt rocks did not yield any clear indication of the presence of such a component, at the level of sensitivity of our method.

Acknowledgments–S. Osae gratefully acknowledges the International Atomic Energy Agency (IAEA) for supporting a postdoctoral fellowship at the University of Vienna. S. Misra thanks the Geological Survey of India, Kolkata, for providing some samples of Lonar impact melt rocks, the Indian Institute of Technology, Kharagpur, for a research associateship, and the Council for Scientific and Industrial Research, New Delhi, for a Senior Research Associateship (grant no. B-10220) for this research work. He is also grateful to the University of Vienna, Austria, for providing a visiting scholarship, and to the Indian Space Research Organization, Bangalore, for providing a grant (No. 9/1/194/2002-II) for Lonar Crater research. We are grateful to Anand Dube, Kolkata, India, for his expert opinion during the progress of this research work. Analytical work was supported by the Austrian Science Foundation, grant P17194-N10 (to C. Koeberl). We are grateful to S. Master (University of the Witwatersrand, Johannesburg), H. Newsom (University of New Mexico), and M. Widdowson (Open University, UK) for detailed and constructive reviews that helped to improve the manuscript, and to W. U. Reimold for his editorial work.

Editorial Handling—Dr. Wolf Uwe Reimold

REFERENCES

Chowdhury A. N. and Handa B. K. 1978. Some aspects of the geochemistry of Lonar lake water. *Indian Journal of Earth Sciences* 5:111–118.

Cox K. G. and Hawkesworth C. J. 1985. Geochemical stratigraphy of the Deccan traps at Mahabaleshwar, Western Ghats, India, with implications for open system magmatic processes. *Journal of Petrology* 26:355–377.

Courtillot V. E. and Renne P. R. 2003. On the ages of flood basalt events. *Comptes Rendus Geosciences* 335:113–140.

Crocket J. H. and Paul D. K. 2004. Platinum-group elements in Deccan mafic rocks: A comparison of suites differentiated by Ir content. *Chemical Geology* 208:273–291.

Feldman V. I., Sazonova L. V., Mironov Y. V., and Kapustkina I. G. 1983. Circular structure Logancha as possible meteorite crater in basalts of the Tunguska syncline (abstract). 14th Lunar and Planetary Science Conference. pp. 191–192.

Floyd P. A. and Winchester J. A. 1978. Identification and discrimination of altered and metamorphosed volcanic rocks using immobile elements. *Chemical Geology* 21:291–306.

Fredriksson K., Dube A., Milton D. J., and Balasundaram M. S. 1973. Lonar Lake, India: An impact crater in basalt. *Science* 180:862–864.

Fredriksson K., Brenner P., Dube A., Milton D., Mooring C., and Nelen J. A. 1979. Petrology, mineralogy, and distribution of Lonar (India) and lunar impact breccias and glasses. *Smithsonian Contributions to the Earth Sciences* 22:1–12.

Fudali R. F. and Fredriksson K. 1992. Tektite-like bodies at Lonar Crater, India? Very unlikely. *Meteoritics* 27:99–100.

Fudali R. R., Milton D. J., Fredriksson K., and Dube A. 1980. Morphology of Lonar Crater, India: Comparison and implications. *The Moon and Planets* 23:493–515.

Ghosh S. and Bhaduri S. K. 2003. Petrography and petrochemistry of impact melts from Lonar crater, Buldana District, Maharashtra, India. *Indian Minerals* 57:1–26.

Grant J. A. 1999. Evaluating the evolution of process specific degradation signatures around impact craters. *International Journal of Impact Engineering* 23:331–340.

Grant J. A. and Schultz P. H. 1993. Degradation of selected terrestrial and martian impact craters. *Journal of Geophysical Research* 98: 11025–11042.

Grieve R. A. F. 1978. The petrochemistry of the melt rocks at Brent Crater and their implication for the condition of impact. *Meteoritics* 13:484–487.

Hagerty J. J. and Newsom H. E. 2003. Hydrothermal alteration at the Lonar Lake impact structure, India: Implications for impact cratering on Mars. *Meteoritics & Planetary Science* 38:365–381.

Irvine T. N. and Baragar W. R. A. 1971. A guide to the chemical classification of the common volcanic rocks. *Canadian Journal of Earth Sciences* 8:523–548.

Kearsley A., Graham G., McDonnell T., Bland P., Hough R., and Helps P. 2004. Early fracturing and impact residue emplacement: Can modelling help to predict their location in major craters? *Meteoritics & Planetary Science* 39:247–265.

Kieffer S. W., Schaal R. B., Gibbons R., Hörz F., Milton D. J., and Dube A. 1976. Shocked basalt from Lonar impact crater, India, and experimental analogues. Proceedings, 7th Lunar Science Conference. pp. 1391–1412.

Koeberl C. 1993. Instrumental neutron activation analysis of geochemical and cosmochemical samples: A fast and proven method for small sample analysis. *Journal of Radioanalytical and Nuclear Chemistry* 168:47–60.

Koeberl C. 1998. Identification of meteoritical components in impactites. In *Meteorites: Flux with time and impact effects*, edited by Grady M. M., Hutchison R., McCall G. J. H., and Rothery D. A. Special Publication #140. London: Geological Society of London. pp. 133–152.

Koeberl C., Reimold W. U., Brandt D., Dallmeyer R. D., and Powell R. A. 1997. Target rocks and breccias from Ames impact structure, Oklahoma: Petrology, mineralogy, geochemistry, and age. In *The Ames structure and similar features*, edited by Johnson K. and Campbell J. Oklahoma Geological Survey Circular #100. Norman: Oklahoma Geological Survey. pp. 169–198.

Koeberl C., Bhandari N., Dhingra D., Suresh P. O., Narasimham V. L., and Misra S. 2004. Lonar impact crater, India: Occurrence of a basaltic suevite? (abstract #1751). 35th Lunar and Planetary Science Conference. (CD-ROM).

Lafond E. C. and Dietz R. S. 1964. Lonar Crater, India, a meteorite crater? *Meteoritics* 2:111–116.

Mahoney J. J. 1988. Deccan traps. In *Continental flood basalts*, edited by Macdougall J. D. Dordrecht: Kluwer Academic Publishing. pp. 151–194.

Malcolmson J. G. 1840. On the fossils of the eastern portion of the great basaltic district of India. *Transactions of the Geological Society of London* 5:537–575.

Maloof A. C., Louzada K. L., Stewart S. T., and Weiss B. P. 2005. Geology of Lonar crater, India: An analog for martian impact craters (abstract #3046). 36th Lunar and Planetary Science Conference. (CD-ROM).

Masaitis V. L. 1999. Impact structures of northeastern Eurasia: The territories of Russia and adjacent countries. *Meteoritics & Planetary Science* 34:691–711.

Mishra S. P. 1987. Lonar Lake and co-linear carbonatites of Western India. *Journal of the Geological Society of India* 29:344–348.

Morgan J. W. 1978. Lonar Crater glasses and high-magnesium australites: Trace element volatilization and meteoritic contamination. Proceedings, 9th Lunar and Planetary Science Conference. pp. 2713–2730.

Murali A. V., Zolensky M. E., and Blanchard D. P. 1987. Tektite-like bodies at Lonar Crater, India: Implications for the origin of tektites. Proceedings, 17th Lunar and Planetary Science Conference. *Journal of Geophysical Research* 92: E729–E735.

Nandy N. C. and Deo V. B. 1961. Origin of the Lonar Lake and its alkalinity. *TISCO* July:144–155.

Nayak V. K. 1972. Glassy objects (impact glasses), a possible new evidence for meteoritic origin of Lonar Crater, Maharashtra State, India. *Earth and Planetary Science Letters* 14:1–6.

Nayak V. K. 1985. Trona in evaporite from the Lonar impact crater, Maharashtra. *Indian Journal of Earth Sciences* 12:221–222.

Nayak V. K. 1993. Maskelynite from the India impact crater at Lonar. *Journal of the Geological Society of India* 41:307–312.

Newbold T. J. 1844. Summary of the Geology of Southern India. *Journal of the Royal Asiatic Society* 12:20–42.

Pandey K. 2002. Age and duration of the Deccan Traps, India: A review of radiometric and paleomagnetic constraints. *Proceedings of the Indian Academy of Sciences (Earth and Planetary Sciences)* 111:1–8.

Pearce J. and Cann J. R. 1973. Tectonic setting of basic volcanic rocks determined using trace element analysis. *Earth and Planetary Science Letters* 19:290–300.

Pearce J. and Norry M. J. 1979. Petrogenetic implications of Ti, Zr, Y, and Nb variations in volcanic rocks. *Contributions to Mineralogy and Petrology* 69:33–47.

Puura V., Huber H., Kirs J., Kärki A., Suuroja K., Kirsimäe K., Kivisilla J., Kleesment A., Konsa M., Preeden U., Suuroja S., and Koeberl C. 2004. Geology, petrography, shock petrography, and geochemistry of impactites and target rocks from the

Kärdla crater, Estonia. *Meteoritics & Planetary Science* 39: 425–452.
Reichow M. K., Saunders A. D., White R. V., Pringle M. S., Al'Mukhamedov A. I., Medvedev A. I., and Kirda N. P. 2002. $^{40}Ar/^{39}Ar$ dates from the West Siberian Basin: Siberian flood basalt province doubled. *Science* 296:1846–1849.
Reimold W. U., Koeberl C., and Bishop J. 1994. Roter Kamm impact crater, Namibia: Geochemistry of basement rocks and breccias. *Geochimica et Cosmochimica Acta* 58:2689–2710.
Roy A. and Chatterjee A. K. 1998. Deccan basalts and its mineralogical alterations in the central and western peninsular India. *Clay Research* 17:72–89.
Sengupta D. 1986. Cosmic ray induced thermoluminescence in moon and meteorites and terrestrial dating applications. Unpublished Ph.D. thesis, Gujarat University, Ahmedabad, India.
Sengupta D. and Bhandari N. 1988. Formation age of the Lonar Crater. 19th Lunar and Planetary Science Conference. pp. 1059–1060.
Sengupta D., Bhandari N., and Watanabe S. 1997. Formation age of Lonar Meteor Crater, India. *Revista de Fisica Aplicada e Instrumentacao* 12:1–7.
Storzer D. and Koeberl C. 2004. Age of the Lonar impact crater, India: First results from fission track dating (abstract #1309). 35th Lunar and Planetary Science Conference. (CD-ROM).
Stroube W. B., Garg A. N., Ali M. Z., and Ehmann W. D. 1978. A chemical study of the impact glasses and basalts from Lonar Crater, India. *Meteoritics* 13:201–208.
Subrahmanyam B. 1985. Lonar Crater, India: A crypto-volcanic origin. *Journal of the Geological Society of India* 26:326–335.
Sukheswala R. N. and Poldervaart A. 1958. Deccan basalts in the Bombay area. *Bulletin of the Geological Society of America* 69: 1475–1494.
Taylor S. R. and McLennan S. M. 1985. *The continental crust: Its composition and evolution.* London: Blackwell. 312 p.
Widdowson M., Walsh J. N., and Subbarao K. V. 1987. The geochemistry of Indian bole horizons: Paleoenvironmental implications of Deccan intravolcanic palaeosurfaces. In *Paleosurfaces: Recognition, reconstruction and palaeoenvironmental interpretation*, edited by Widdowson M. Special Publication 210. London: Geological Society. pp. 269–281.
Widdowson M., Pringle M. S., and Fernandez O. A. 2000. A post K-T boundary (early Palaeocene) age for Deccan-type feeder dykes, Goa, India. *Journal of Petrology* 41:1177–1194.

APPENDIX

Table A1. Locations and field-based sample classifications (cf. Fig. 1b).

Location	Sample details
1	Soil sample with impact melt spherules
2	Soil sample with impact melt spherules
3	Soil sample with impact melt spherules
4	Possible impact melt rock (not in-situ)
5	Basalt flow (possible lower most flow)
6	Impact melt rocks (not in-situ)
6X	Impact melt rock (not in-situ)
7	Shocked basalt (?)
8	Impact melt rock (not in-situ)
9	Upper most basalt flow in the Lonar crater
10	Basalt flow below the uppermost flow
11	Basalt flow second next to the upper most flow
12	Impact melt rock (not in-situ)
13	Area where impact melts and spherules are strewn over the paddy field
14	Uppermost basalt flow
15	Second basalt flow from top
16	Third basalt flow from top
17	Ejecta blanket location
18	Soil sample with impact melt spherules
19	Basalt flow (no sample collected)
20	Basalt flow (no sample collected)
21	Basalt flow
22	Possible homogeneous impact melt
23	Ejecta spherules (impact melt?)
24	Impact melt (non in-situ)
25	Weathered samples of basalt
26	Impact melt rock (not in-situ)
27	Impact melt rock (not in-situ)
28	Ejecta spherules (impact melt)

Table A1. *Continued.* Locations and field-based sample classifications (cf. Fig. 1b).

Location	Sample details
29	Impact melt rock (homogeneous)
30	Soil sample with impact melt spherules
31	Ejecta spherules (impact melt)
32	Weathered impact melt rock
33	Basalt flow
34	Basalt flow
35	Basalt flow (near location 8)
36	Impact melt rock
37	Fragment of impact melt rock
38	Basalt flow
39	Ejecta spherule
40	Basalt flow
41	Basalt flow
42	Basalt flow
43	Basalt flow
44	Ejecta spherule or fragment of impact melt
IM	Impact melt rock, homogeneous
CF-1	Basalt flow no. 1
CF-2	Basalt flow no. 2
CF-3	Basalt flow no. 3
CF-4	Basalt flow no. 4
CF-5	Basalt flow no. 5
CF-6	Basalt flow no. 6
GSI-1	Impact melt rock, homogeneous
D-1 and D-2	Impact melt spherules

Samples 1-IM collected by S. Misra (2000-2003); sample GSI-1 from Geological Survey of India, Kolkata; CF samples collected by S. Gosh; samples D1 and D-2 collected by D. Sengupta. Classification of samples according to glass/melt rock "types" discussed in the text: type a: DSG-1/A, 1/B, 1/C, 1/E, 1/F, 1/G and 1/H; type b: L-44, L-13B; type c: GSI-1, SG-1, SG-2, SG-3, L-22, L-23, L-29; type 'd': L-27A, L-36, L-37X; type e: L-7; type f: L-4, L-6a, L-6b, L-8.